Cell Stem Cell

Daily light and darkness cues regulate bone marrow stem and progenitor cell maintenance and blood replenishment

--Manuscript Draft--

Manuscript Number:	CELL-STEM-CELL-D-17-00527R2
Full Title:	Daily light and darkness cues regulate bone marrow stem and progenitor cell maintenance and blood replenishment
Article Type:	Research Article
Keywords:	hematopoietic stem and progenitor cells; light/darkness; TNF; ROS; melatonin; norepinephrine; Bone marrow; differentiation and egress; maintenance and retention; vascular permeability; stem cell repopulation potential.
Corresponding Author:	Tsvee Lapidot, Ph.D. Weizmann Institute of Science Rehovot, - ISRAEL
First Author:	Karin Golan, PhD
Order of Authors:	Karin Golan, PhD
	Anju Kumari, PhD
	Orit Kollet, PhD
	Eman Khatib-Massalha, MSc
	Mohana Devi Subramaniam, PhD
	Zulma S. Ferreira, PhD
	Francesca Avemaria, PhD
	Sylwia Rzeszotek, PhD
	Andrés García-García, PhD
	Stephanie Xie, PhD
	Eugenia Flores-Figueroa, PhD
	Shiri Gur-Cohen, PhD
	Tomer Itkin, PhD
	Aya Ludin-Tal, PhD
	Hassan Massalha, PhD
	Biana Bernshtein, MSc
	Andrzej K. Ciechanowicz, PhD
	Alexander Brandis, PhD
	Tevie Mehlman, PhD
	Suditi Bhattacharya, MSc
	Mayla Bertagna, MSc
	Hui Cheng, PhD
	Ekaterina Petrovich-Kopitman, PhD
	Tomasz Janus, PhD
	Nathali Kaushansky, PhD
	Tao Cheng, MD

Powered by Editorial Manager® and ProduXion Manager® from Aries Systems Corporation

	Irit Sagi, PhD
	Mariusz Z. Ratajczak, MD/PhD
	Simón Méndez-Ferrer, PhD
	John E. Dick, PhD
	Regina P. Markus, PhD
	Tsvee Lapidot, PhD
Abstract:	Intensive daily production of mature leukocytes and blood replenishment by hematopoietic stem and progenitor cells (HSPC), while maintaining the bone marrow (BM) reservoir of undifferentiated long-term repopulating hematopoietic stem cells (LT-HSC) are tightly coordinated. How light and darkness regulate these dynamic needs is poorly understood. We identified two daily BM HSPC peaks initiated by light and darkness onset. Both peaks are following transient elevations of BM norepinephrine (NE) and TNF secretion, temporarily increasing HSPC reactive oxygen species (ROS) levels. Morning elevated NE and TNF augmented BM HSPC differentiation, increased vascular permeability and blood replenishment. Nocturnal melatonin facilitated CD150high expression, LT-HSC function and BM maintenance, directly and indirectly via increased COX-2/αSMA macrophages, diminished vascular permeability, and reduced HSPC ROS levels. Our study reveals physiologic daily light and darkness BM NE and TNF bursts, essential for synchronized mature blood cell production and melatonin primed BM HSPC repopulation potential with suggestive clinical relevance.

Powered by Editorial Manager® and ProduXion Manager® from Aries Systems Corporation

Manuscript

Daily light and darkness cues regulate bone marrow stem and progenitor cell maintenance and blood replenishment

Karin Golan[1], Anju Kumari[1], Orit Kollet[1], Eman Khatib-Massalha[1], Mohana-Devi Subramaniam[1], Zulma S. Ferreira[2], Francesca Avemaria[1], Sylwia Rzeszotek[3], Andrés García-García[4], Stephanie Xie[5], Eugenia Flores-Figueroa[5,6], Shiri Gur-Cohen[1], Tomer Itkin[1], Aya Ludin-Tal[1], Hassan Massalha[7], Biana Bernshtein[1], Andrzej K. Ciechanowicz[8], Alexander Brandis[9], Tevie Mehlman[9], Suditi Bhattacharya[1], Mayla Bertagna[1], Hui Cheng[1,10], Ekaterina Petrovich-Kopitman[9], Tomasz Janus[11], Nathali Kaushansky[1], Tao Cheng[10], Irit Sagi[12], Mariusz Z. Ratajczak[13], Simón Méndez-Ferrer[4], John E. Dick[5], Regina P. Markus[2] and Tsvee Lapidot[1,14,*]

[1]Immunology Dept., [7]Molecular cell biology Dept., [9]Life Science Core Facilities, [12]Biological Regulation Dept., Weizmann Institute of Science, Rehovot, Israel
[2] Physiology Dept., University of São Paulo, São Paulo, Brazil
[3]Physiology Dept., [11]Forensic Medicine Dept., Pomeranian Medical University, Szczecin, Poland
[4]Haematology Dept., University of Cambridge, Cambridge, UK
[5]Princess Margaret Cancer Centre, University Health Network, Toronto, Ontario, Canada.
[6]Oncology Research Unit, Oncology Hospital, National Medical Center Century XXI, IMSS, Mexico City, Mexico.
[8]Regenerative Medicine Dept., University of Warsaw, Warsaw, Poland
[10] State Key Laboratory of ExperimantalHematology, Institute of hematology and Blood Disease Hospital, Chinese Academy of Medical Sciences and Peking Union Medical College, Tianjin, China
[13]Stem Cell Institute, University of Louisville, Louisville, KY, USA
[14]Lead Contact
*Correspondence: Tsvee.Lapidot@weizmann.ac.il

Summary

Intensive daily production of mature leukocytes and blood replenishment by hematopoietic stem and progenitor cells (HSPC), while maintaining the bone marrow (BM) reservoir of undifferentiated long-term repopulating hematopoietic stem cells (LT-HSC) are tightly coordinated. How light and darkness regulate these dynamic needs is poorly understood. We identified two daily BM HSPC peaks initiated by light and darkness onset. Both peaks are following transient elevations of BM norepinephrine (NE) and TNF secretion, temporarily increasing HSPC reactive oxygen species (ROS) levels. Morning elevated NE and TNF augmented BM HSPC differentiation, increased vascular permeability and blood replenishment. Nocturnal melatonin facilitated $CD150^{high}$ expression, LT-HSC function and BM maintenance, directly and indirectly via increased COX-2/αSMA macrophages, diminished vascular permeability, and reduced HSPC ROS levels. Our study reveals physiologic daily light and darkness BM NE and TNF bursts, essential for synchronized mature blood cell production and melatonin primed BM HSPC repopulation potential with suggestive clinical relevance.

Introduction

Bone marrow (BM) residing hematopoietic stem and progenitor cells (HSPC) intensively produce and replenish the blood daily with new mature blood and immune cells with a finite lifespan, while preserving the pool of undifferentiated stem cells including long-term repopulating hematopoietic stem cells (LT-HSC). Shifting between these dual HSPC functions is regulated by signals originating from various cell types residing in the BM microenvironment and by external light/dark cycles (Mendelson and Frenette, 2014; Yu and Scadden, 2016). These signals activate HSPC regulating their metabolism and function. Increased reactive oxygen species (ROS) is a major regulator of HSPC migration and development (Ludin et al., 2014) (Ludin et al., 2012). Light/dark cycles are translated by neural and hormonal cues including sympathetic output and melatonin and are implicated in bone turnover (Fu et al., 2005; Simmons and Nichols, 1966), host immunity and inflammation (Curtis et al., 2014; Man et al., 2016) (Borniger et al., 2017), and neutrophil clearance (Casanova-Acebes et al., 2013).

HSPC egress from the BM to the blood is regulated by elevated morning NE release by the nervous system in response to daylight and reduced BM CXCL12 levels (Lucas et al., 2008; Mendez-Ferrer et al., 2008). HSPC egress is also regulated daily by corticosterone (Kollet et al., 2013) and complement activation (Borkowska et al., 2016). The balance between BM CXCL12 and blood sphingosine 1-phosphate (S1P), dynamically regulate HSPC recruitment to the circulation versus their BM retention (Golan et al., 2013).

Tumor necrosis factor (TNF) is a major inflammatory cytokine, which is mostly secreted by activated leukocytes in a daily rhythm manner (Arjona and Sarkar, 2005; Bissonnette et al., 1995). TNF also regulates HSPC which functionally express its receptors (Dybedal et al., 2001; Pronk et al., 2011; Rezzoug et al., 2008). The darkness hormone, melatonin is synthesized by the pineal gland and by BM cells (Mias et al., 2008), exerting anti-oxidative and immunomodulatory functions (Carrillo-Vico et al., 2013).

To reveal how the BM HSPC reservoir is maintained we examined the kinetics of daily light and dark cues and revealed major players involved. We identified two major daily BM HSPC peaks (morning and night) with different function. The morning peak increased HSPC proliferation, differentiation, egress, and blood replenishment while the night peak mediated HSPC maintenance and replenishment of the BM stem cell pool.

Results

Light and dark mediated BM HSPC proliferation peaks are driven by TNF and ROS elevations

To understand how daily 11 A.M HSPC release peak (Mendez-Ferrer et al., 2008) lead to BM stem cell reservoir replenishment, we measured BM HSPC levels along 24 hours (**Figure 1A**). We identified two major BM HSPC peaks, at 11AM and 11PM, preceded by two minor peaks at 7AM and at 7PM, (**Figure 1B**) accompanied by lower levels of

quiescent G_0 HSPC, implicating cell proliferation (**Figure 1C**). Examination of primitive BM $CD34^-$/LSK HSPC at 4h intervals confirmed similar daily waves (**Figure 1D**). Since activated HSPC have higher reactive oxygen species (ROS) content than quiescent HSPC (Itkin et al., 2016; Ludin et al., 2014; Takizawa et al., 2017), we traced ROS expression in BM $CD34^-$LSK cells along the day. An oscillating pattern of ROS^{high}/$CD34^-$LSK cells increment at 7AM and at 7PM (**Figures 1E and 1F**) preceding the HSPC peaks, suggested that ROS elevation promotes their proliferation, inducing small HSPC subsets to cycle at 11AM and at 11PM. Mice treatment with a ROS scavenger, N-Acetyl Cysteine (NAC), following initiation or termination of light led to reduced BM $CD34^-$ LSK cells levels (**Figures 1G and 1H**). We looked for factors that may elevate ROS levels. BM-residing HSPC are regulated by inflammatory cytokines activating stress signals (Schuettpelz and Link, 2013; Trumpp et al., 2010) among them tumor necrosis factor (TNF), which is also implicated in their activation (Cabezas-Wallscheid et al., 2017). Mice treated with TNF to activate their HSPC had elevated levels of ROS^{high}/$CD34^-$LSK cells in the BM 4h later (**Figures 1I and 1J**). Tracking BM TNF levels revealed two daily peaks, a higher one at 7AM and a modest one at 7PM (**Figure 1K**), suggesting light and dark induced TNF involvement in BM HSPC regulation.

TNF bursts are essential for BM HSPC peaks

We tested the levels of the TNF converting enzyme (TACE), which cleaves TNF from the plasma membrane of cells to its active form (Black et al., 1997). TACE levels fluctuated both on BM HSPC (**Figure 2A**) and on monocytes (**Figure S1A**). We found two peaks of TACE elevations specific for HSPC, corresponding to the 7AM and 7PM BM TNF peaks. Next, we administered a TACE inhibitor (Sagi, 2015) to mice after initiation or termination of light and found reduced BM HSPC peaks (**Figures 2B and 2C**). We further utilized a genetic model of TNF knockout (KO) mice and also treated wild-type (WT) mice with a TNF antagonist. No oscillations were observed in BM CFU-C of TNF KO mice as compared to WT mice **(Figure 2D)**. Moreover, both peaks of BM HSPC documented in WT mice at 11AM and 11 PM were decreased in these mice (**Figures 2E-2H**). Antagonizing TNF during the morning revealed higher levels of BM HSPC in their quiescent phase of the cell cycle at 11AM **(Figure S1B).** Interestingly, TNF deficiency also prevented the daily ROS peaks in BM HSPC (**Figure 2I**), suggesting that TNF bursts are crucial for HSPC ROS oscillations. We established chimeric mice with WT hematopoietic cells transplanted into TNF KO mice and vice versa and found that the hematopoietic and not stromal compartment is responsible for TNF secretion and HSPC ROS regulation at 7AM (**Figure 2J**) (**Figure 2K**). TNF activates NF-kB signaling cascades (Morgan and Liu, 2011), which regulate HSPC, in particular p65 (canonical pathway) is essential for HSC function (Stein and Baldwin, 2013) while RelB (non-canonical pathway) regulates HSC development (Zhao et al., 2012). We found higher levels of phosphorylated p65 and RelB molecules in HSPC at 7AM compared with 7PM (**Figures 2L-2M**). Utilizing TNF KO mice or TNF antagonist

treatment led to reduced p65- and RelB-phosphorylation at 7AM and 7PM in BM HSPC (**Figures 2L-2M**). Altogether, suggesting that TNF signaling is important for the two major BM HSPC peaks.

Light and darkness onset induce transient TNF bursts via NE up-regulation.

To determine if light/dark signals modulate TNF levels, we scored this cytokine concentration. Profound transient changes in TNF levels were observed 1h after transferring mice from light to darkness in both BM and plasma, which were back to basal levels following 2h (**Figures 3A and S1C**). A similar trend was documented upon transferring mice from darkness to light (**Figures 3B and S1D**). Since norepinephrine (NE) signaling regulates BM HSPC egress at 11 A.M (Mendez-Ferrer et al., 2008), we monitored its levels and found that BM NE peaked at 7AM and to a lower extent at 7PM, similar to the TNF bursts (**Figures 3C and S1E**). Blockage of β2- or β3-adrenoreceptors (β2AR or β3AR) following light initiation, showed that β2AR but not β3AR antagonist reduced TACE levels on BM HSPC and monocytes, decreasing TNF levels at 7AM (**Figures 3D-3G and S1F**). Accordingly, mice deficient of β2AR ($\beta2AR^{-/-}$) or both β2AR and β3AR ($\beta2AR^{-/-}/\beta3AR^{-/-}$) but not β3AR only, had reduced BM TNF levels at 7AM (**Figure 3H**). Moreover, inhibition of β2AR reduced TACE levels on BM HSPC and monocytes and decreased TNF levels also at 7PM (**Figures 3I-3L**). Both NE and TNF induce ROS elevation in cells. Therefore, we treated mice with NAC to scavenge ROS following initiation or termination of light and found reduced TACE levels on BM HSPC and monocytes as well as decreased BM TNF levels at 7AM and at 7PM (**Figures 3D-G,-I-L**). Further studying the cross talk between NE and TNF revealed higher basal NE levels in TNF KO mice and WT mice treated with TNF antagonist (**Figure S1G**), suggesting a negative feedback loop. We administered NE at a HSPC mobilizing dose (Dar et al., 2011) and found that TNF KO mice were unable to mobilize HSPC (**Figure S1I**) despite high sensitivity to PBS injections, which elevated circulating white blood cells (WBC) (**Figure S1H**). These results suggest that upon light induction or termination, stress reactions activate the sympathetic nerve system to increase TACE on BM HSPC and monocytes via NE and β2AR, leading to BM TNF elevations which induce both HSPC peaks.

The morning HSPC peak regulates differentiation and egress while the night peak regulates retention

To learn the two HSPC peaks function, we examined short and long-term (LT) HSPC repopulation potential. BM cells harvested at 11AM and 11PM were transplanted in competitive repopulation assays (**Figure 4A**). Despite high BM HSPC content at 11AM (**Figures 1B and 1D**), these cells had inferior short and long-term repopulation activity, compared to 11 PM BM HSPC (**Figures 4B-4C**). Importantly primitive BM

$CD150^{+}/CD34^{-}$/LSK LT-HSC peaked only at 11PM (**Figures 4D-4E and S2A**) accompanied by reduced c-kit expression (**Figure S2B**), which is associated with increased HSC serial repopulation potential (Grinenko et al., 2014). These results reveal that the two major HSPC peaks are phenotypically and functionally different.

Since LT-HSC fluctuations cannot be explained by the limited proliferation of CD34-LSK cells, we tested if light and dark cues change their phenotype and function by dynamic changes in cell surface antigen expression. We found higher $CD150^{high}$ levels of expression on $CD34^{-}$LSK cells at 11PM compared to 11AM (**Figure S2C**). Next, we prevented light induction at 6AM maintaining mice under extended dark conditions up to 11AM which maintained higher $CD150^{+}/CD34^{-}$/LSK LT-HSC levels at 11AM (**Figures 4F and S2D**) and increased $CD150^{high}$ levels of expression on $CD34^{-}$LSK cells (**Figures S2E**). We also tested whether the 11PM peak of LT-HSC depends on TNF by applying a TNF antagonist following light termination and found reduced $CD150^{+}/CD34^{-}$/LSK LT-HSC levels at 11PM (**Figures 4G and S2F**). At 11AM we documented higher levels of common myeloid progenitors (CMP), common lymphoid progenitors (CLP), neutrophils, monocytes and lymphocytes. In contrast at 11PM, we found no elevations in these immature and mature populations (**Figures 4H-4M**, respectively). Since HSPC differentiation and egress are linked to ROS elevation, (Golan et al., 2012; Ludin et al., 2014; Suda et al., 2011) we measured the levels of circulating HSPC, which indicate their egress from the BM. Egress was high during the morning HSPC peak (11AM) and low at night (**Figures 4N-4O**), corroborating previous reports (Mendez-Ferrer et al., 2008). Moreover, mature leukocyte egress was also increased during the morning HSPC peak **(Figures S2G and S2H)**. More permeable BM sinusoidal blood vessels are the major site for HSPC trafficking from and to the BM (Itkin et al., 2016). We measured BM vascular permeability and found higher permeability at 11AM in line with the extended cell egress (**Figure 4P**). Another regulator of lymphocyte and of HSPC egress and mobilization is the bio-active lipid S1P (Pappu et al., 2007) (Golan et al., 2012; Juarez et al., 2012; Ratajczak et al., 2010). Measuring S1P levels in the plasma revealed higher levels of S1P during the morning compared to the night (**Figure S2I**). In accordance, higher S1P levels at night were measured in the BM (**Figure S2J**), further suggesting BM HSPC retention. In summary, during the 11 AM morning peak, HSPC are primed to a state of high differentiation and egress, imposing lower repopulation potential. In contrast, during the 11 PM night peak HSPC are primed to a state of retention with low differentiation and high BM reservoir replenishment including LT-HSC, imposing high repopulation potential.

Elevated morning BM NE levels facilitate vascular permeability, HSPC differentiation and egress

HSPC egress and trafficking is regulated by NE (Mendez-Ferrer et al., 2008; Scheiermann et al., 2012; Spiegel et al., 2007). Blockage of β3-AR **(Figure 5A)** reduced

HSPC CMP and CLP differentiation (**Figures 5B and 5C**), and mature Mac-1^+ neutrophils and monocytes (**Figures S3A-S3C**). In line, β3-antagonist also reduced BM vascular permeability (**Figure 5D**) decreasing HSPC (**Figures 5E and S3D**) and mature leukocyte egress at 11AM (**Figures S3E and S3F**). Administration of β3-antagonist following light initiation increased HSPC repopulation potential (**Figures 5F and S3G**) and elevated $CD150^+/CD34^-$/LSK levels (**Figure 5G**). Next we tested CMP and CLP levels and HSPC egress in TNF KO and WT mice treated with TNF antagonist at 11AM. Both mouse models had reduced BM CMP and CLP levels and decreased HSPC egress to the circulation (**Figures 5H-5K,** respectively and **S3H**). When we treated mice with NE at light termination (**Figure 5L),** it induced ROS elevation (**Figures 5M-5N and S3I**). Moreover, NE injection (**Figure 5O**) enhanced the levels of BM CMP (**Figures 5P and S3J**) and CLP (**Figures 5Q and S3K**), BM vascular permeability (**Figures 5R and S3L)** and HSPC egress to the circulation (**Figures 5S and S3M-S3N**). These results reveal that light-induced NE elevation in the BM leads to increased TACE expression, TNF shedding via β2AR on BM leukocytes, induction of HSPC differentiation and egress and increased BM vascular permeability via β3AR.

Melatonin retains undifferentiated HSPC in the BM during the night peak.

Melatonin is present in the BM and is also produced by BM cells (Carrillo-Vico et al., 2013; Conti et al., 2000; Tan et al., 1999). By measuring melatonin levels in plasma and BM fluids we found the highest levels at night (11PM) (**Figures 6A and 6B**). TNF inhibits melatonin production in the pineal gland (Fernandes et al., 2006), but induces its production by macrophages (Muxel et al., 2012). Interestingly, TNF KO mice or mice treated with its antagonist had lower BM melatonin levels at 11PM (**Figure 6C**). Injection of the melatonin antagonist luzindole (**Figure 6D**) at night, induced HSPC differentiation (**Figures 6E-6F and S4A-S4B**), increased BM vascular permeability (**Figure 6G)** and HSPC egress to the circulation (**Figures 6H and S4C**). Similarly, luzindole induced release of neutrophils and monocytes (**Figures S4D and S4E**). Melatonin injection in the morning (**Figure 6I**), reduced ROS levels in BM $CD34^-$LSK cells (**Figures 6J-6K**) and their CMP and CLP differentiation (**Figures 6L-6M**). Melatonin administration also reduced BM vascular permeability (**Figure 6N)** and HSPC egress to the circulation (**Figures 6O and S4F**) at 11AM. Since we found elevated LT-HSC function during nocturnal melatonin secretion (**Figure 4C**), we examined if more primitive phenotype of $Flt3^-/CD34^-$/SLAM/LSK **is** also elevated at night. Indeed, we report increased BM $Flt3^-/CD34^-$/SLAM/LSK levels at 11PM as compared to 11AM (**Figures 6P and S4G-S4H**). Importantly, melatonin administration at 6AM also augmented $Flt3^-/CD34^-$/SLAM/LSK levels (**Figures 6Q and S4I**) including elevated $CD150^{high}$ surface expression at 11AM (**Figures S4J**) and increased competitive short term repopulation (**Figures 6R**). Preliminary results reveal that *in vivo* administration of melatonin following light initiation up-regulated human LT-HSC and to a lower extent

ST-HSC phenotypes but not the more differentiated MPL (**Figure S4K-S4M**) in human stem cell engrafted immune-deficient chimeric mice. These results reveal similar trends for mice and humans with regards to melatonin regulation of HSPC. Of note, C57BL/6 mice have lower melatonin production by the pineal gland but high melatonin levels in the BM (Conti et al., 2000). To exclude strain specific phenotypes we tested C3H/HeN mice with normal melatonin levels and documented similar patterns of HSPC ROS levels, BM HSPC peaks, increase in 11PM LT-HSC, and 11AM differentiation and egress (**Figures S5A-G**). Both MT1 and MT2 melatonin receptors are expressed on BM CD34-LSK HSPC (**Figure 6S**). Upon binding of melatonin to its receptors, several molecular pathways can be activated or repressed, among them Akt (Blask et al., 2014). We treated BM cells *in vitro* with melatonin for 10 min and found reduced Akt phosphorylation (**Figure 6T**). Since Akt activation increase HSPC ROS levels (Ludin et al., 2012), we treated Lin^- enriched HSPC with melatonin and found reduced ROS levels in BM HSPC (**Figure 6U**). These results suggest that melatonin can directly regulate BM HSPC retention in a low metabolic state during the night peak.

Melatonin elevates BM COX-2/αSMA macrophages

Rare COX-2/αSMA macrophages preserve BM HSPC by reducing their ROS levels (Ludin et al., 2012). We detected the highest levels of BM αSMA macrophages at 11PM (**Figures 7A and S5G**). Importantly, their COX-2 expression was also enhanced (**Figure 7B**), revealing their activated state. These cells express MT1 and MT2 melatonin receptors (**Figures 7C and S6A-S6B**). Enforced morning melatonin elevation (**Figure 7D**) up-regulated BM αSMA macrophage levels (**Figure 7E**). Interestingly, melatonin reduced αSMA macrophage G_0 phase of the cell-cycle (**Figure 7F**) and increased their ROS levels (**Figure 7G**). Moreover, melatonin also decreased αSMA macrophage egress to the circulation (**Figure S6C**). Accordingly, melatonin receptor inhibition by luzindole (**Figure 7H**) reduced BM αSMA macrophages levels at 11PM (**Figure 7I**), increased their G_0 cell-cycle phase (**Figure 7J**) and reduced their ROS levels (**Figure 7K**). Since, melatonin treatment did not increase COX-2 expression (**Figure S6D**) and as S1P increases COX-2 expression in smooth muscle cells (Hsieh et al., 2006), and since BM S1P levels increase during the night **(Figure S2H)**, our data suggests that the augmented S1P levels in the BM induce nocturnal COX-2 elevation. Next, we inhibited COX-2 activity in mice by using a specific inhibitor at night to abolish the regulatory effect of this enzyme (**Figure 7L**), which did not reduce the population of BM COX-2/αSMA macrophages (**Figure S6E**). This treatment enhanced HSPC CMP and CLP differentiation (**Figures 7M and 7N, respectively and S6F-S6G**), and their egress to the circulation (**Figures 7O and S6H-S6I**). Furthermore, COX-2 inhibition during the night elevated ROS levels in immature HSPCs (**Figures 7P-7Q and S6J**) and decreased primitive $CD150^+/CD34^-$/LSK LT-HSC levels (**Figures 7R and S6K**). Finally, we utilized CX3CR1/DTR mice in which we ablated $CX3CR1^+$ monocytes and macrophages

(Diehl et al., 2013). Since COX-2 αSMA macrophages express this receptor (Ludin et al., 2012), their levels were decreased upon administration of Diphtheria toxin to these mice (**Figure 7S**). Interestingly, we also found reduced levels of primitive $CD150^{+}/CD34^{-}$ /LSK LT-HSC levels at 11PM, in these mice (**Figures 7T and S6L**). Our data reveals how melatonin directly and indirectly via αSMA macrophages, maintains undifferentiated BM HSPC including with LT-HSC function during the night.

Discussion

In this study we identified daily fluctuations driven by light/dark signals, which regulate BM HSPC. Light-induction initiates sympathetic signals inducing egress of BM HSPC including LT-HSC (Casanova-Acebes et al., 2013; Mendez-Ferrer et al., 2008). We found in the morning enhanced BM HSPC proliferation and differentiation, including CLP and CMP elevations prior to their egress. Consequently, the BM requires daily replenishment with new immature and maturing cells to allow continuous homeostatic balance between ongoing demands of mature blood cell production while maintaining the reservoir of undifferentiated stem and progenitor cells. Thus, our results reveal during the day replenishment of the circulation with immature and mature leukocytes while at night the BM pool of stem and progenitor cells is replenished.

We identified two major BM HSPC peaks at 11AM and 11PM, in line with a previous report (Ieyasu et al., 2014). Our data suggests that BM HSPC are metabolically programmed by day-light NE induced signals for their differentiation and egress accompanied by reduced repopulation potential. These BM HSPC are metabolically reprogrammed at night by dark-signals to reacquire their undifferentiated state, accompanied by elevated repopulation potential. The night HSPC state is a result of limited HSPC proliferation but more due to dynamic changes in cell surface antigen expression and metabolic state induced by melatonin. Surface CXCR4 fluctuates between day and night (Mendez-Ferrer et al., 2008) and surface LT-HSC EPCR is shed by TACE and is later re-expressed in the BM (Gur-Cohen et al., 2015). Overall, light-induced HSPC migration and development versus dark-induced optimal LT-HSC function recovery on a daily basis suggest tight regulation of HSC state and readiness to rapidly act upon demand. Thus homeostatic regulation maintain and "train" HSC for emergency acute stress situations when their function is critical for rapid production of mature blood and immune cells while maintaining the stem cell reservoir in order to prevent hematology failure (Gur-Cohen et al 2015).

HSPC, including LT-HSC functionally express TNF receptors and are regulated by TNF released during infection onset (King and Goodell, 2011; Trumpp et al., 2010). In line, TNF promoted BM-regeneration (Bowers et al., 2018). We identified two BM TNF daily

bursts following light initiation/termination. Restricting TNF genetically or pharmacologically abolished daily peaks, attributing a pivotal role to TNF in BM HSPC regulation. TNF burst decodes the environmental information of light on/off transitions, which may serve as a transient physiological stress, preparing BM HSPC for their sequential activation. Light/dark induction elevated BM NE, which acts directly on leukocytes to increase TACE expression leading to TNF cleavage.

Daylight raised NE, reduced BM CXCL12 and induced $CXCR4^{+}$ HSPC egress (Lucas et al., 2008; Mendez-Ferrer et al., 2008). Antagonizing either β3AR or TNF signaling inhibited the morning peak, reduced vascular permeability, HSPC differentiation and egress. NE treatment induced rapid murine HSPC mobilization (Dar et al., 2011) and human peripheral blood myeloid cell differentiation, associated with ROS production (Liu et al., 2015). Although ROS is rapidly elevated by NE and TNF 7AM morning peak, the outcome of this process is evident only a few hours later in terms of differentiation and egress.

Intriguingly, the high 7AM morning NE and TNF bursts facilitated HSPC differentiation and egress while their lower 7PM night bursts induced limited HSPC proliferation without differentiation and egress. These dual effects suggest multi factorial regulation. The major night peak is predominantly driven by elevation of BM melatonin, which together with COX-2/αSMA macrophages and reduced endothelial cell permeability, inhibited HSPC differentiation and egress. In support of our study, CD8/TCR cells enhanced HSPC-engraftment by TNF-dependent regulation (Rezzoug et al., 2008). Melatonin protected circulating human HSPC from chemotherapy via ROS down-regulation (Carrillo-Vico et al., 2013) and human BM stromal cells from toxicity (Mehrzadi et al., 2017).

COX-2/αSMA macrophages support BM HSPC retention by lowering their ROS levels (Ludin et al., 2012). These cells functionally express melatonin receptors and peak at night in response to melatonin. Antagonizing melatonin signaling or inhibiting COX-2 at night turned the BM to a morning-like phenotype. Interestingly, partial deletion of $COX\text{-}2^{high}$/αSMA macrophages from the BM, reduced LT-HSC levels, further demonstrating the importance of these cells in HSPC BM maintenance.

Our study demonstrates tightly synchronized balance of BM NE, TNF, COX-2 and melatonin to maintain mature leukocyte homeostasis. Basal inflammatory signals are required for steady state HSC function (King and Goodell, 2011). Of interest, LPS induced HSPC proliferation directly via their TLR4 following a short stimulation. However, longer exposure impaired HSC competitive self-renewal and repopulation (Takizawa et al., 2017), demonstrating the need for robust short pulses of pro-inflammatory signals rather than chronic stimulations which impair stem cell function.

We found dynamic oscillations of the BM homeostatic milieu of cytokines/hormones/neurotransmitters which are crucial for maintaining the dual activity

of HSPC: replenishing the blood with new mature cells with a finite life span on demand while maintaining the BM reservoir of undifferentiated stem and progenitor cells.
Our preliminary results reveal similar effects of melatonin on human HSPC including LT-HSC. This data suggest that the time of BM HSPC harvest and transplantation may impact engraftment and repopulation efficiency in clinical BM transplantation. These results also suggest that manipulations with light and dark cues, melatonin, NE, COX-2 and TNF could improve clinical stem cell transplantation protocols.

Acknowledgments
We thank Prof. David Wallach for providing TNF KO mice and for fruitful discussions.
We also thank Prof. Steffen Jung for the CX3CR1/DTR mice, for fruitful discussions and for critically reviewing the results with these mice. This work was funded by The São Paulo Research Foundation (FAPESP), Brazil/Weizmann Institute of Science, Israel, joint research projects (FAPESP/Weizmann Grant - 2015/50166-8) (T.L., R.P.M); A research grant from the Dr. Beth Rom-Rymer Stem Cell Research Fund (T.L.); The Canadian Institutes of Health Research (CIHR), the International Development Research Centre (IDRC), the Israel Science Foundation (ISF) and the Azrieli Foundation (T.L.); The Ernest and Bonnie Beutler Research Program of Excellence in Genomic Medicine (T.L.); The ISF-NSFC joint research program (2474/16) (T.L.); and research grants from the Pertman Fund for Stem Cell Research and the Mashkin Family Foundation (T.L.); CAMS Initiative for Innovative Medicine (2016-I2M-1-017) and CAMS Fundamental Research Funds for Central Research Institutes (2016GH3100001). (T.C.).

Author Contributions
K.G. designed and performed experiments, analyzed data and wrote the manuscript; A.K dedicatedly helped with experiments throughout the day and night and critically reviewed the MS, O.K helped in the design and execution of experiments and wrote the manuscript; E.K.M helped in the design and execution of experiments; M.D.S dedicatedly helped with experiments and summarized data; Z.S.F designed and performed experiments related to melatonin; F.A, S.G.C, T.I, N.K, A.L.T, H.M, S.B, EPK and M.B helped with experiments; S.R, A.K.C and T.J performed experiments related to S1P and NE (method #1); A.G.G performed experiments related to TNF levels in β2AR and β3AR deficient mice; S.X and K.F (visiting scientist in the lab of J.E.D) performed experiments related to β3AR antagonist and human xenografts treated with melatonin; B.B helped with experiments related to iDTR mice; A.B and T.M performed experiments related to NE (method #2); H.C helped with experiments related to vascular permeability; T.C, M.Z.R, S.M.F, and J.E.D critically reviewed the manuscript; I.S developed and provided us with the specific TACE inhibitor; R.P.M designed experiments related to melatonin, helped with writing of the manuscript and critically reviewed it; T.L. supervised and designed the research and wrote the manuscript.

Declaration of Interests:
The authors declare no competing interests.

References:
Arjona, A., and Sarkar, D.K. (2005). Circadian oscillations of clock genes, cytolytic factors, and cytokines in rat NK cells. J Immunol *174*, 7618-7624.

Bahr, C., von Paleske, L., Uslu, V.V., Remeseiro, S., Takayama, N., Ng, S.W., Murison, A., Langenfeld, K., Petretich, M., Scognamiglio, R., *et al.* (2018). A Myc enhancer cluster regulates normal and leukaemic haematopoietic stem cell hierarchies. Nature *553*, 515-520.

Bissonnette, E.Y., Enciso, J.A., and Befus, A.D. (1995). Inhibition of tumour necrosis factor-alpha (TNF-alpha) release from mast cells by the anti-inflammatory drugs, sodium cromoglycate and nedocromil sodium. Clin Exp Immunol *102*, 78-84.

Black, R.A., Rauch, C.T., Kozlosky, C.J., Peschon, J.J., Slack, J.L., Wolfson, M.F., Castner, B.J., Stocking, K.L., Reddy, P., Srinivasan, S., *et al.* (1997). A metalloproteinase disintegrin that releases tumour-necrosis factor-alpha from cells. Nature *385*, 729-733.

Blask, D.E., Dauchy, R.T., Dauchy, E.M., Mao, L., Hill, S.M., Greene, M.W., Belancio, V.P., Sauer, L.A., and Davidson, L. (2014). Light exposure at night disrupts host/cancer circadian regulatory dynamics: impact on the Warburg effect, lipid signaling and tumor growth prevention. PloS one *9*, e102776.

Borkowska, S., Suszynska, M., Ratajczak, J., and Ratajczak, M.Z. (2016). Evidence of a Pivotal Role for the Distal Part of the Complement Cascade in the Diurnal Release of Hematopoietic Stem Cells Into Peripheral Blood. Cell transplantation *25*, 275-282.

Borniger, J.C., Walker Ii, W.H., Gaudier-Diaz, M.M., Stegman, C.J., Zhang, N., Hollyfield, J.L., Nelson, R.J., and DeVries, A.C. (2017). Time-of-Day Dictates Transcriptional Inflammatory Responses to Cytotoxic Chemotherapy. Sci Rep *7*, 41220.

Boughton, B.A., Callahan, D.L., Silva, C., Bowne, J., Nahid, A., Rupasinghe, T., Tull, D.L., McConville, M.J., Bacic, A., and Roessner, U. (2011). Comprehensive profiling and quantitation of amine group containing metabolites. Anal Chem *83*, 7523-7530.

Bowers, E., Slaughter, A., Frenette, P.S., Kuick, R., Pello, O.M., and Lucas, D. (2018). Granulocyte-derived TNFalpha promotes vascular and hematopoietic regeneration in the bone marrow. Nat Med *24*, 95-102.

Cabezas-Wallscheid, N., Buettner, F., Sommerkamp, P., Klimmeck, D., Ladel, L., Thalheimer, F.B., Pastor-Flores, D., Roma, L.P., Renders, S., Zeisberger, P., *et al.* (2017). Vitamin A-Retinoic Acid Signaling Regulates Hematopoietic Stem Cell Dormancy. Cell *169*, 807-823 e819.

Carrillo-Vico, A., Lardone, P.J., Alvarez-Sanchez, N., Rodriguez-Rodriguez, A., and Guerrero, J.M. (2013). Melatonin: buffering the immune system. Int J Mol Sci *14*, 8638-8683.

Casanova-Acebes, M., Pitaval, C., Weiss, L.A., Nombela-Arrieta, C., Chevre, R., N, A.G., Kunisaki, Y., Zhang, D., van Rooijen, N., Silberstein, L.E., *et al.* (2013). Rhythmic modulation of the hematopoietic niche through neutrophil clearance. Cell *153*, 1025-1035.

Conti, A., Conconi, S., Hertens, E., Skwarlo-Sonta, K., Markowska, M., and Maestroni, J.M. (2000). Evidence for melatonin synthesis in mouse and human bone marrow cells. J Pineal Res *28*, 193-202.

Curtis, A.M., Bellet, M.M., Sassone-Corsi, P., and O'Neill, L.A. (2014). Circadian clock proteins and immunity. Immunity *40*, 178-186.

Dar, A., Schajnovitz, A., Lapid, K., Kalinkovich, A., Itkin, T., Ludin, A., Kao, W.M., Battista, M., Tesio, M., Kollet, O., *et al.* (2011). Rapid mobilization of hematopoietic progenitors by AMD3100 and catecholamines is mediated by CXCR4-dependent SDF-1 release from bone marrow stromal cells. Leukemia *25*, 1286-1296.

Diehl, G.E., Longman, R.S., Zhang, J.X., Breart, B., Galan, C., Cuesta, A., Schwab, S.R., and Littman, D.R. (2013). Microbiota restricts trafficking of bacteria to mesenteric lymph nodes by CX(3)CR1(hi) cells. Nature *494*, 116-120.

Dybedal, I., Bryder, D., Fossum, A., Rusten, L.S., and Jacobsen, S.E. (2001). Tumor necrosis factor (TNF)-mediated activation of the p55 TNF receptor negatively regulates maintenance of cycling reconstituting human hematopoietic stem cells. Blood *98*, 1782-1791.

Fernandes, P.A., Cecon, E., Markus, R.P., and Ferreira, Z.S. (2006). Effect of TNF-alpha on the melatonin synthetic pathway in the rat pineal gland: basis for a 'feedback' of the immune response on circadian timing. J Pineal Res *41*, 344-350.

Fu, L., Patel, M.S., Bradley, A., Wagner, E.F., and Karsenty, G. (2005). The molecular clock mediates leptin-regulated bone formation. Cell *122*, 803-815.

Golan, K., Kollet, O., and Lapidot, T. (2013). Dynamic Cross Talk between S1P and CXCL12 Regulates Hematopoietic Stem Cells Migration, Development and Bone Remodeling. Pharmaceuticals *6*, 1145-1169.

Golan, K., Vagima, Y., Ludin, A., Itkin, T., Cohen-Gur, S., Kalinkovich, A., Kollet, O., Kim, C., Schajnovitz, A., Ovadya, Y., *et al.* (2012). S1P promotes murine progenitor cell egress and mobilization via S1P1-mediated ROS signaling and SDF-1 release. Blood *119*, 2478-2488.

Grinenko, T., Arndt, K., Portz, M., Mende, N., Gunther, M., Cosgun, K.N., Alexopoulou, D., Lakshmanaperumal, N., Henry, I., Dahl, A., *et al.* (2014). Clonal expansion capacity

defines two consecutive developmental stages of long-term hematopoietic stem cells. J Exp Med *211*, 209-215.

Gur-Cohen, S., Itkin, T., Chakrabarty, S., Graf, C., Kollet, O., Ludin, A., Golan, K., Kalinkovich, A., Ledergor, G., Wong, E., *et al.* (2015). PAR1 signaling regulates the retention and recruitment of EPCR-expressing bone marrow hematopoietic stem cells. Nat Med *21*, 1307-1317.

Hsieh, H.L., Wu, C.B., Sun, C.C., Liao, C.H., Lau, Y.T., and Yang, C.M. (2006). Sphingosine-1-phosphate induces COX-2 expression via PI3K/Akt and p42/p44 MAPK pathways in rat vascular smooth muscle cells. J Cell Physiol *207*, 757-766.

Ieyasu, A., Tajima, Y., Shimba, S., Nakauchi, H., and Yamazaki, S. (2014). Clock gene Bmal1 is dispensable for intrinsic properties of murine hematopoietic stem cells. J Negat Results Biomed *13*, 4.

Itkin, T., Gur-Cohen, S., Spencer, J.A., Schajnovitz, A., Ramasamy, S.K., Kusumbe, A.P., Ledergor, G., Jung, Y., Milo, I., Poulos, M.G., *et al.* (2016). Distinct bone marrow blood vessels differentially regulate haematopoiesis. Nature *532*, 323-328.

Juarez, J.G., Harun, N., Thien, M., Welschinger, R., Baraz, R., Pena, A.D., Pitson, S.M., Rettig, M., DiPersio, J.F., Bradstock, K.F., *et al.* (2012). Sphingosine-1-phosphate facilitates trafficking of hematopoietic stem cells and their mobilization by CXCR4 antagonists in mice. Blood *119*, 707-716.

King, K.Y., and Goodell, M.A. (2011). Inflammatory modulation of HSCs: viewing the HSC as a foundation for the immune response. Nat Rev Immunol *11*, 685-692.

Kollet, O., Dar, A., Shivtiel, S., Kalinkovich, A., Lapid, K., Sztainberg, Y., Tesio, M., Samstein, R.M., Goichberg, P., Spiegel, A., *et al.* (2006). Osteoclasts degrade endosteal components and promote mobilization of hematopoietic progenitor cells. Nat Med *12*, 657-664.

Kollet, O., Vagima, Y., D'Uva, G., Golan, K., Canaani, J., Itkin, T., Gur-Cohen, S., Kalinkovich, A., Caglio, G., Medaglia, C., *et al.* (2013). Physiologic corticosterone oscillations regulate murine hematopoietic stem/progenitor cell proliferation and CXCL12 expression by bone marrow stromal progenitors. Leukemia *27*, 2006-2015.

Liu, Y., Wei, J., Guo, G., and Zhou, J. (2015). Norepinephrine-induced myeloid-derived suppressor cells block T-cell responses via generation of reactive oxygen species. Immunopharmacol Immunotoxicol *37*, 359-365.

Lucas, D., Battista, M., Shi, P.A., Isola, L., and Frenette, P.S. (2008). Mobilized hematopoietic stem cell yield depends on species-specific circadian timing. Cell Stem Cell *3*, 364-366.

Ludin, A., Gur-Cohen, S., Golan, K., Kaufmann, K.B., Itkin, T., Medaglia, C., Lu, X.J., Ledergor, G., Kollet, O., and Lapidot, T. (2014). Reactive oxygen species regulate

hematopoietic stem cell self-renewal, migration and development, as well as their bone marrow microenvironment. Antioxidants & redox signaling *21*, 1605-1619.

Ludin, A., Itkin, T., Gur-Cohen, S., Mildner, A., Shezen, E., Golan, K., Kollet, O., Kalinkovich, A., Porat, Z., D'Uva, G., *et al.* (2012). Monocytes-macrophages that express alpha-smooth muscle actin preserve primitive hematopoietic cells in the bone marrow. Nat Immunol.

Man, K., Loudon, A., and Chawla, A. (2016). Immunity around the clock. Science *354*, 999-1003.

Mehrzadi, S., Safa, M., Kamrava, S.K., Darabi, R., Hayat, P., and Motevalian, M. (2017). Protective mechanisms of melatonin against hydrogen-peroxide-induced toxicity in human bone-marrow-derived mesenchymal stem cells. Can J Physiol Pharmacol *95*, 773-786.

Mendelson, A., and Frenette, P.S. (2014). Hematopoietic stem cell niche maintenance during homeostasis and regeneration. Nat Med *20*, 833-846.

Mendez-Ferrer, S., Lucas, D., Battista, M., and Frenette, P.S. (2008). Haematopoietic stem cell release is regulated by circadian oscillations. Nature *452*, 442-447.

Mias, C., Trouche, E., Seguelas, M.H., Calcagno, F., Dignat-George, F., Sabatier, F., Piercecchi-Marti, M.D., Daniel, L., Bianchi, P., Calise, D., *et al.* (2008). Ex vivo pretreatment with melatonin improves survival, proangiogenic/mitogenic activity, and efficiency of mesenchymal stem cells injected into ischemic kidney. Stem Cells *26*, 1749-1757.

Morgan, M.J., and Liu, Z.G. (2011). Crosstalk of reactive oxygen species and NF-kappaB signaling. Cell research *21*, 103-115.

Muxel, S.M., Pires-Lapa, M.A., Monteiro, A.W., Cecon, E., Tamura, E.K., Floeter-Winter, L.M., and Markus, R.P. (2012). NF-kappaB drives the synthesis of melatonin in RAW 264.7 macrophages by inducing the transcription of the arylalkylamine-N-acetyltransferase (AA-NAT) gene. PloS one *7*, e52010.

Pappu, R., Schwab, S.R., Cornelissen, I., Pereira, J.P., Regard, J.B., Xu, Y., Camerer, E., Zheng, Y.W., Huang, Y., Cyster, J.G., *et al.* (2007). Promotion of lymphocyte egress into blood and lymph by distinct sources of sphingosine-1-phosphate. Science *316*, 295-298.

Pronk, C.J., Veiby, O.P., Bryder, D., and Jacobsen, S.E. (2011). Tumor necrosis factor restricts hematopoietic stem cell activity in mice: involvement of two distinct receptors. J Exp Med *208*, 1563-1570.

Ratajczak, M.Z., Lee, H., Wysoczynski, M., Wan, W., Marlicz, W., Laughlin, M.J., Kucia, M., Janowska-Wieczorek, A., and Ratajczak, J. (2010). Novel insight into stem cell mobilization-plasma sphingosine-1-phosphate is a major chemoattractant that directs the egress of hematopoietic stem progenitor cells from the bone marrow and its level in

peripheral blood increases during mobilization due to activation of complement cascade/membrane attack complex. Leukemia *24*, 976-985.

Rezzoug, F., Huang, Y., Tanner, M.K., Wysoczynski, M., Schanie, C.L., Chilton, P.M., Ratajczak, M.Z., Fugier-Vivier, I.J., and Ildstad, S.T. (2008). TNF-alpha is critical to facilitate hemopoietic stem cell engraftment and function. J Immunol *180*, 49-57.

Sagi, I., Wong, E. & Afik, R. (2015). Variants of TACE pro-domain as TNF-A inhibitor and their medical use. US patent 20150132281 A1.

Scheiermann, C., Kunisaki, Y., Lucas, D., Chow, A., Jang, J.E., Zhang, D., Hashimoto, D., Merad, M., and Frenette, P.S. (2012). Adrenergic nerves govern circadian leukocyte recruitment to tissues. Immunity *37*, 290-301.

Schuettpelz, L.G., and Link, D.C. (2013). Regulation of hematopoietic stem cell activity by inflammation. Front Immunol *4*, 204.

Simmons, D.J., and Nichols, G., Jr. (1966). Diurnal periodicity in the metabolic activity of bone tissue. Am J Physiol *210*, 411-418.

Spiegel, A., Shivtiel, S., Kalinkovich, A., Ludin, A., Netzer, N., Goichberg, P., Azaria, Y., Resnick, I., Hardan, I., Ben-Hur, H., *et al.* (2007). Catecholaminergic neurotransmitters regulate migration and repopulation of immature human CD34+ cells through Wnt signaling. Nat Immunol *8*, 1123-1131.

Stein, S.J., and Baldwin, A.S. (2013). Deletion of the NF-kappaB subunit p65/RelA in the hematopoietic compartment leads to defects in hematopoietic stem cell function. Blood *121*, 5015-5024.

Suda, T., Takubo, K., and Semenza, G.L. (2011). Metabolic regulation of hematopoietic stem cells in the hypoxic niche. Cell Stem Cell *9*, 298-310.

Takizawa, H., Fritsch, K., Kovtonyuk, L.V., Saito, Y., Yakkala, C., Jacobs, K., Ahuja, A.K., Lopes, M., Hausmann, A., Hardt, W.D., *et al.* (2017). Pathogen-Induced TLR4-TRIF Innate Immune Signaling in Hematopoietic Stem Cells Promotes Proliferation but Reduces Competitive Fitness. Cell Stem Cell.

Tan, D.X., Manchester, L.C., Reiter, R.J., Qi, W.B., Zhang, M., Weintraub, S.T., Cabrera, J., Sainz, R.M., and Mayo, J.C. (1999). Identification of highly elevated levels of melatonin in bone marrow: its origin and significance. Biochim Biophys Acta *1472*, 206-214.

Trumpp, A., Essers, M., and Wilson, A. (2010). Awakening dormant haematopoietic stem cells. Nat Rev Immunol *10*, 201-209.

Wolf, Y., Boura-Halfon, S., Cortese, N., Haimon, Z., Sar Shalom, H., Kuperman, Y., Kalchenko, V., Brandis, A., David, E., Segal-Hayoun, Y., *et al.* (2017). Brown-adipose-

tissue macrophages control tissue innervation and homeostatic energy expenditure. Nat Immunol *18*, 665-674.

Yu, V.W., and Scadden, D.T. (2016). Heterogeneity of the bone marrow niche. Curr Opin Hematol *23*, 331-338.

Zhao, C., Xiu, Y., Ashton, J., Xing, L., Morita, Y., Jordan, C.T., and Boyce, B.F. (2012). Noncanonical NF-kappaB signaling regulates hematopoietic stem cell self-renewal and microenvironment interactions. Stem Cells *30*, 709-718.

Figure legends:

Figure 1: **Light and darkness cues induce two peaks of BM HSPC proliferation via TNF and ROS production. (A)** Illustration of the daylight/darkness zeitgeber time and its equivalent hours of the day. **(B)** BM CFU-C at different time points of the day (*n* = 8). **(C)** Percentage of quiescent G_0 stage of BM $CD34^-$/LSK cells (*n* = 5). **(D)** Numbers of BM $CD34^-$/LSK cells per femur (*n* = 8). **(E-F)** Representative Fluorescence-activated cell sorting (FACS) analysis of ROS^{high} within $CD34^-$LSK cells (E) and summarized data (F, *n* = 7) of the percentage of ROS^{high} $CD34^-$LSK cells in the BM. Representative experiment out of four. **(G-H)** Schematic illustrations of NAC administration protocol (G). Numbers of BM $CD34^-$/LSK cells per femur in control and NAC treated mice in the morning (H, *n* = 4) and night (H, *n* = 4). **(I-J)** FACS analysis (I) of BM ROS^{high} $CD34^-$ LSK cells and the summarized data (J, *n* = 4) 4h following TNF administration. **(K)** BM TNF levels at different time points of the day (*n* = 6). Error bars, mean ± s.e.m. *P < 0.05; **P < 0.01; ***P < 0.001; ****P < 0.0001, Student's two-tailed unpaired t-test (J), one-way ANOVA with Tukey's *post hoc* test (B-D, F, H, K).

Figure 2: **TNF is essential for HSPC BM peaks induction. (A)** BM TACE level of expression in $CD34^-$/LSK cells (*n* = 5). **(B-C)** Schematic illustrations of TACE inhibitor administration protocol (B). Numbers of BM $CD34^-$/LSK cells per femur in control and TACE inhibitor treated mice in the morning (C, *n* = 4) and night (C, *n* = 4). **(D)** Number of BM CFU-C of WT (*n* = 6) and TNF KO (*n* = 5) mice. **(E-H)** Schematic illustrations of TNF antagonist administration protocol in the morning (E) or night (G). Numbers of BM $CD34^-$/LSK cells per femur in WT and TNF KO mice and TNF antagonist treated mice in the morning (F, *n* = 5) and night (H, *n* = 6). **(I)** Percentage of ROS^{high} $CD34^-$LSK cells in the BM of WT (*n* = 5) and TNF KO (*n* = 4) mice. **(J)** TNF levels in the BM (*n* = 4) of chimeric mice: WT into TNF KO or TNF KO into WT as compared to BM TNF levels of WT and TNF KO mice. **(K)** Percentage of ROS^{high} $CD34^-$LSK cells in the BM (*n* = 4) of WT into TNF KO or TNF KO into WT chimeric mice and compared to WT and TNF KO mice. **(L-M)** Percentage of phosphorylated p65 (L, *n* = 4) or RelB (M, *n* = 4) in BM $CD34^-$LSK cells at 7AM and 7PM in control and TNF KO (at 7AM only) and in mice

treated with the TNF antagonist. Error bars, mean ± s.e.m. *P < 0.05; **P < 0.01; ***P < 0.001; ****P < 0.0001, One-way ANOVA with Tukey's *post hoc* test. See also figure S1.

Figure 3: **TNF is transiently elevated via NE secretion following light and darkness onset. (A)** TNF levels in the BM (*n* = 4) following 1h or 2h switch from light to darkness. **(B)** TNF levels in the BM (*n* = 4) following 1h or 2h switch from darkness to light. **(C)** NE levels in the BM (*n* = 6) at different time points of the day. **(D-G)** Schematic illustrations of β2AR antagonist or NAC treatment protocol in the morning (D). BM TACE level of expression in $CD34^-$/LSK cells (E, *n* = 4) or monocytes (F, *n* = 5) following β2AR antagonist or NAC administration. TNF levels in the BM (G, *n* = 5) at 7AM following β2AR antagonist or NAC administration. **(H)** TNF levels in the BM (*n* = 5) measured by ELISA (Milliplex) in β2AR receptor KO mice ($\beta2AR^{-/-}$), β3AR KO mice ($\beta3AR^{-/-}$) and $\beta2AR^{-/-}$/ $\beta3AR^{-/-}$ double KO mice. **(I-L)** Schematic illustrations of β2AR antagonist or NAC administration protocol at evening (I). BM TACE level of expression in $CD34^-$/LSK cells (J, *n* = 4) or monocytes (K, *n* = 4) at 7PM following β2AR antagonist or NAC administration. TNF levels in the BM (L, *n* = 4) at 7PM following β2AR antagonist or NAC administration. Error bars, mean ± s.e.m. *P < 0.05; **P < 0.01; ***P < 0.001; ****P < 0.0001, One-way ANOVA with Tukey's *post hoc* test. See also figure S1.

Figure 4: **The daylight peak involves increased egress and differentiation while the night peak consists of retention and reduced differentiation. (A)** Schematic illustration of BM competitive transplantation. **(B-C)** Short-term (B, *n* = 6, 4 weeks) and long-term (C, *n* = 5, 16 weeks) repopulation ability of WT BM cells. **(D-E)** FACS representative plots (D) and data summarize (E, *n* = 5) of the number of BM $CD150^+/CD34^-$/LSK cells per femur. **(F)** Numbers of BM $CD150^+/CD34^-$/LSK cells per femur at 11AM in mice exposed to extended darkness (*n* = 5). **(G)** Numbers of BM $CD150^+/CD34^-$/LSK cells per femur at 11PM in mice treated with TNF antagonist (*n* = 4). **(H)** FACS analysis strategy for BM common myeloid progenitor (CMP) and common lymphoid progenitor (CLP) cells. **(I-J)** Numbers of BM CMP cells (I, *n* = 7) or CLP cells (J, *n* = 8) per femur. **(K-M)** Numbers of BM Neutrophils (G, *n* = 9), monocytes (H, *n* = 6) and lymphoid (I, *n* = 6) cells per femur **(N-O)** FACS representative plots (N) and the numbers of circulating LSK cells per ml of blood (O, *n* = 8). **(P)** Levels of BM Evans Blue Dye absorbance per femur at 620nm in mice (*n* = 4). Error bars, mean ± s.e.m. *P < 0.05; **P < 0.01; ***P < 0.001; ****P < 0.0001, Student's two-tailed unpaired t-test (B-C, F-G, P), one-way ANOVA with Tukey's *post hoc* test (E, I-M, O). See also figure S2.

Figure 5: **Elevated morning NE further increaseROS levels and vascular permeability leading to HSPC egress and differentiation. (A)** Schematic illustrations of β3AR antagonist administration protocol. **(B-E)** Number of BM CMP (B, *n* = 6) or CLP (C, *n* = 6) cells per femur, Evans Blue Dye absorbance per femur at 620 nm (D, *n* =

4) and circulating LSK cells per ml of blood (E, *n* = 8) following β3AR antagonist administration. **(F)** Long-term (*n* = 5, 16 weeks) repopulation ability of BM cells from mice treated with the β3AR antagonist, harvested at 11AM and transplanted to WT recipient mice. **(G)** Numbers of BM $CD150^{+}/CD34^{-}$/LSK cells per femur at 11AM in mice treated with β3AR antagonist (*n* = 4). **(H)** Schematic illustrations of TNF antagonist administration protocol. **(I-K)** Number of BM CMP (I, *n* = 4) or CLP (J, *n* = 6) cells per femur and circulating LSK cells per ml of blood (K, *n* = 5) in WT and TNF KO mice and TNF antagonist treated mice. **(L-N)** Schematic illustrations of a single NE injection protocol related to panel (L). FACS analysis (M) of BM ROS^{high} $CD34^{-}$LSK cells and the summarized data (N, *n* = 4) following NE 1h administration. **(O-S)** Schematic illustration of NE double injection protocol related to panels P-S (O). **N**umber of BM CMP (P, *n* = 5) or CLP (Q, *n* = 6) cells per femur, Evans Blue Dye absorbance per femur at 620nm (R, *n* = 4) and circulating LSK cells per ml of blood (S, *n* = 8) in NE treated mice at night. Error bars, mean ± s.e.m. *P < 0.05; **P < 0.01; ***P < 0.001; ****P < 0.0001, Student's two-tailed unpaired t-test (B-G, N-S), one-way ANOVA with Tukey's *post hoc* test (I-K). See also figure S3.

Figure 6: **During the night augmented melatonin levels maintain HSPC undifferentiated and retained in the BM. (A-B)** Melatonin levels in the plasma (A, *n* = 7) and BM (B, *n* = 4) at different time points of the day. **(C)** Melatonin levels in the BM (*n* = 6) at 11PM in TNF KO mice and WT mice treated with TNF antagonist. **(D-H)** Schematic illustrations of melatonin inhibitor (luzindole) administration protocol (D). Number of BM CMP (E, *n* = 5) or CLP (F, *n* = 4) cells per femur, Evans Blue Dye absorbance per femur at 620nm (G, *n* = 5) and circulating LSK cells per ml of blood (H, *n* = 6) following luzindole administration. **(I-O)** Schematic illustrations of melatonin administration protocol (I). FACS analysis (J) of BM ROS^{high} $CD34^{-}$LSK cells and the summarized data (K, *n* = 5) following melatonin administration. Number of BM CMP (L, *n* = 4) or CLP (M, *n* = 4) cells per femur, Evans Blue Dye absorbance per femur at 620nm (N, *n* = 4) and circulating LSK cells per ml of blood (O, *n* = 5) in melatonin treated mice in the morning. **(P)** Numbers of BM $Flt3^{-}/CD34^{-}$/SLAM/LSK cells per femur at 11AM and 11PM (*n* = 4). **(Q)** Numbers of BM $Flt3^{-}/CD34^{-}$/SLAM/LSK cells per femur at 11AM in mice treated with melatonin versus control vehicle treated mice (*n* = 5). **(R)** Short-term (*n* = 6 for PBS (x=full dose), *n* = 7 for melatonin (x=full dose) *n* = 5 for melatonin (1/2x=half dose), 4 weeks) repopulation ability of WT BM cells from control and mice treated with melatonin in the morning like in the schematic illustration (I). **(S)** FACS representative plots of the levels of MT1 and MT2 melatonin receptors in BM $CD34^{-}$/LSK cells at 7PM. **(T)** Phosphorylated Akt levels in $CD34^{-}$/LSK cells 10 min following in vitro stimulation with melatonin (*n* = 7). **(U)** Percentage of ROS^{high} $CD34^{-}$ LSK cells following 1h in vitro stimulation of Lineage negative cells with melatonin (*n* = 4). Error bars, mean ± s.e.m. *P < 0.05; **P < 0.01; ***P < 0.001; ****P < 0.0001,

Student's two-tailed unpaired t-test (E-S), one-way ANOVA with Tukey's *post hoc* test (A-C). See also figures S4 and S5.

Figure 7: **Melatonin-induced elevation of COX-2/αSMA macrophages to indirectly reduce HSPC egress and differentiation. (A)** Numbers of BM αSMA/Mac-1 macrophages per femur at different time points of the day (*n* = 9). **(B)** Levels of COX-2 expression in BM αSMA/Mac-1 macrophages (*n* = 5). **(C)** FACS representative plots of the levels of MT1 and MT2 melatonin receptors in BM αSMA/Mac-1 macrophages at 7PM. **(D-G)** Schematic illustrations of melatonin administration protocol (D). Number of BM αSMA/Mac-1 macrophages per femur (E, *n* = 5) at 11AM following melatonin administration. Percentage of quiescent G_0 stage of BM αSMA/Mac-1 macrophages at 11AM following melatonin administration (F, *n* = 4). Percentage of ROS^{high} BM αSMA/Mac-1 macrophages cells at 11AM following melatonin administration (G, *n* = 5). **(H-K)** Schematic illustrations of luzindole administration protocol (H). Number of BM αSMA/Mac-1 macrophages per femur (I, *n* = 5) at 11PM following luzindole administration. Percentage of quiescent G_0 stage of BM αSMA/Mac-1 macrophages at 11PM following luzindole administration (J, *n* = 4). Percentage of ROS^{high} BM αSMA/Mac-1 macrophages cells at 11PM following luzindole administration (K, *n* = 5). **(L-O)** Schematic illustrations of COX-2 inhibitor administration protocol (L). Number of BM CMP (M, *n* = 4) or CLP (N, *n* = 6) cells per femur and circulating LSK cells per ml of blood (O, *n* = 6) following COX-2 inhibitor administration. **(P-Q)** FACS analysis (P) of ROS expression in BM $CD34^-$/LSK cells and the summarized data (Q, *n* = 5) for the percentage of ROS^{high} $CD34^-$LSK cells in the BM following COX-2 inhibitor administration. **(R)** Numbers of BM $CD150^+/CD34^-$/LSK cells per femur at 11PM following COX-2 inhibitor administration (*n* = 4). **(S-T)** Percentage of BM $COX\text{-}2^{high}$ αSMA/Mac-1 macrophages (S, *n* = 5) and numbers of BM $CD150^+/CD34^-$/LSK cells per femur (T, *n* = 5) at 11PM following 12h depletion of Cx3cr1 monocyte and macrophages in DTR mice (+/- mice contain the diphtheria toxin receptor for the depletion). Error bars, mean ± s.e.m. *P < 0.05; **P < 0.01; ***P < 0.001, Student's two-tailed unpaired t-test (E-S), one-way ANOVA with Tukey's *post hoc* test (A-B). See also figure S6.

STAR methods

- **CONTACT FOR REAGENT AND RESOURCE SHARING**

As the Lead Contact, Tsvee Lapidot (Weizmann Institute of Science, Rehovot, Israel) is responsible for all reagent and resource requests. Please contact Tsvee Lapidot at Tsvee.Lapidot@weizmann.ac.il with requests and inquiries.

- **EXPERIMENTAL MODEL AND SUBJECT DETAILS**

Mice

C57BL/6 (CD45.2) and C3H/HeN mice were purchased from Harlan Laboratories (Rehovot, Israel). B6.SJL (CD45.1) mice were bred at the Weizmann Institute of Science. Breeding and all experimental procedures were monitored by the Veterinary Resources Unit of the Weizmann Institute and were approved by the Institutional Animal Care and Use Committee (IACUC). TNF-KO mice were purchased from Jackson Laboratory (strain#005540) by the group of Prof. David Wallach (Weizmann Institute) and bred at Weizmann Institute. These mice were kindly provided to us. Cx3cr1/DTR mice were kindly given to us by Prof. Steffen Jung (Weizmann Institute). These mice were generated by crossing Cx3cr1stop-DTR (Jackson Laboratory strain # 025629) to Pgk1-Cre (Jackson Laboratory strain # 020811). The progeny express DTR in all Cx3cr1 expressing cells (Diehl et al., 2013). β2 adrenergic receptor KO ($\beta2AR^{-/-}$, *Adrb2tm1Bkk/J*), β3 adrenergic receptor KO ($\beta3AR^{-/-}$, $Adrb3^{tm1Lowl}$) and double KO of β2 and β3 adrenergic receptors ($\beta2AR^{-/-}$/ $\beta3AR^{-/-}$) mice were bred at the university of Cambridge. $\beta2AR^{-/-}$/ $\beta3AR^{-/-}$ mice were obtained by breeding from single KO strains.

All transgenic mice with homozygous mutations were compared to strain matched wild-type C57BL/6 sex- and age-matched controls. 8–12-week-old mice, both male and female, were used for all experiments, keeping the same gender for each experiment. Mice were housed in a standard 12/12 light/dark cycles, ZT0 light on, ZT12 light off. Mice sacrificed at 7PM or 11PM mice were acclimatized for 2 weeks and kept in a room with inverse light/dark cycles to enable working during the day with mice under the dark period. Exceptional is measuring TNF levels after light switch on and off. The mice were either switched from light to darkness at 2PM for 1 or 2 hours or from dark to light at 2AM for 1 or 2 hours. These time points have been selected in order to avoid effects driven by the physiologic TNF elevation and HSPC peaks. Moreover, in the experiments of extended darkness, we keep the mice under dark continuously after the normal 12h of dark up to 11AM. These mice were sacrificed still in the dark, preventing them exposure to light between 6AM to 11AM. Bone marrow cells were obtained by flushing long bones with PBS, and peripheral blood was collected from the heart using heparinized syringes. White blood cell (WBC) counts in the circulation were determined after red blood cell lysis.

Xenogeneic models and human data

Animal experiments were done in accordance to the institutional guidelines approved by the University Health Network animal care committee. NSG female mice (NOD.Cg *Prkdc*scid*Il2rg*tm1Wjl /SzJ; Jackson Laboratory) or NSG-SGM3 female mice (NOD-scid IL2Rgnull-3/GM/SF; Jackson Laboratory) were sub-lethally irradiated with 250 Rad 24 hours before intrafemoral injection with 100,000 Lin^- human cord blood (CB) cells. Xenografts were treated at 4 weeks post-transplantation with vehicle control (EtOH) or melatonin (0.75mg/kg freshly dissolved in vehicle from Sigma) by peritoneal injection at the start of light at 6AM and then euthanized at 10AM for human chimerism analysis. The injected femur and non-injected femur were collected and crushed in Iscove's modified Dulbecco's medium and human chimerism and HSPC populations were assessed as described in the flow cytometry section above.

- **METHOD DETAILS**

In vivo treatments

For circadian studies, mice were sacrificed 1h (7AM) and 5h (11AM) after light initiation at 6AM or 1h (6PM) and 5h (11PM) after light termination at 6PM. TNF was purchased from PeproTech (cat # 300-01A, Human recombinant TNF) and was injected intraperitoneally at 5µg/mouse for 4h before cells were harvested at 11PM.

TACE monomeric prodomain inhibitor was developed and produced as previously described (Sagi, 2015). The TACE inhibitor was used *in vivo* and administrated intravenously at 25 µg/mouse at 6AM to inhibit BM HSPC peak at 11AM or at 12.5 µg/mouse 6PM to inhibit BM HSPC peak at 11PM. TNF antagonist was purchased from Calbiochem (cat #654255) and was injected intraperitoneally at 10µg/mouse twice, at 6AM and 9AM, to inhibit the morning HSPC peak at 11AM or at 5µg/mouse once at 6PM to inhibit the night HSPC peak at 11PM. N-Acetyl Cystein (NAC) was purchased from Sigma (cat # A8199) and was injected intraperitoneally at 25mg/kg at 6AM to monitor TACE and TNF levels at 7AM or to inhibit 11AM BM HSPC peak. NAC was administered at 10mg/kg at 6PM to monitor TACE and TNF levels at 7PM or to inhibit 11PM BM HSPC peak.

β3 antagonist (SR58894A) was purchased from Sigma (cat # SML0581) and was injected intraperitoneally at 10mg/kg twice, at 6AM and 9AM, to inhibit the morning HSPC peak at 11AM. β3 antagonist was also injected intraperitoneally at 20mg/kg at 5AM to monitor TACE and TNF levels at 7AM. β2 antagonist (ICI) was purchased from Sigma (cat # I127) and was injected intraperitoneally at 5mg/kg at 6AM or at 6PM to monitor TACE and TNF levels at 7AM or 7PM respectively. NE was purchased from Sigma (cat # A9512) and was injected intraperitoneally at 10mg/kg twice, at 6PM and 9PM, to modify the night HSPC peak at 11PM. NE was also injected at 2PM (10mg/kg) to induce mobilization in WT and TNF KO mice at 3PM. Luzindole was purchased from Sigma

(cat #L2407) and was injected intraperitoneally at 2.5mg/kg once at 6PM to inhibit the night HSPC peak at 11PM. Melatonin was purchased from Sigma (cat #M5250) and was injected intraperitoneally at 0.75mg/kg once at 6AM to modify the morning HSPC peak at 11AM. COX-2 inhibitor (NS398) was purchased from Sigma (cat #N194) and was injected intraperitoneally at 10mg/kg twice at 6PM and 9PM to inhibit the night HSPC peak at 11PM.

Flow cytometry

Cell populations were analyzed with a FACSCalibur instrument (Becton-Dickinson) or with a MacsQuant instrument (Miltenyi, Bergisch Gladbach, Germany) or with a FACS LSRII (BD Biosciences) with FACSDiva software. Data were analyzed with CellQuest or MacsQuant or FlowJo respectively. Flushed bone marrow cells were stained for 30 minutes at 4°C in flow cytometry buffer (PBS, 10% FCS and 0.02% azide). For antigens that require intracellular staining (αSMA macrophages, Ki67, COX-2, MT1 and MT2 melatonin receptors, phosphorylated RelB or p65, phosphorylated Akt), cell surface staining was followed by cell fixation and permeabilization with the Cytofix/Cytoperm kit (BD Biosciences) according to the manufacturer's instructions. For LSK ($Lin^-/Sca\text{-}1^+/c\text{-}Kit^+$) staining, we used a lineage cocktail of either FITC-conjugated antibodies to CD4 (GK1.5), CD8 (53–6.7), B220 (RA3-6B2), CD11b (M1/70), Gr-1 (RB6-8C5) and Ter119 (TER-119) (all from Biolegend) or a biotinylated lineage cocktail (Miltenyi), together with anti Sca-1-PE (D7) or Sca-1-PE-Cy7 (D7) and anti c-Kit-APC (2B8) (all from Biolegend). As secondary conjugated antibody we used Streptavidin-PE-Cy7 (Biolegend). For CD34/LSK ($Lin^-/Sca\text{-}1^+/c\text{-}Kit^+/CD34^-$), CD34 expression on LSK cells was analyzed using anti CD34-eFlour 450 (RAM34, eBiosciences) or CD34- biotinylated (RAM34, eBioscience). Since currently there are different strategies described in the literature to gate for primitive BM stem cell populations, we applied two strategies: staining for CD150+/CD34-/LSK cells as previously described by de Lecea and Weismann et al (**Figure S2A**) or more stringent staining for Flt3-/CD34-/SLAM (CD150+CD48-)/LSK cells as previously described by the laboratories of Morrison and Trumpp (**Figure S4G**). For $CD150^+/CD34^-$/LSK ($CD150^+/CD34^-/Lin^-/Sca\text{-}1^+/c\text{-}Kit^+$), CD150 expression on $CD34^-$/LSK cells was analyzed using anti CD150-VioGreen (TC15-12F12.2, Biolegend). For $Flt3^-/CD34^-$/SLAM/LSK ($Flt3^-/CD34^-/CD150^+/CD48^-/Lin^-/Sca\text{-}1^+/c\text{-}Kit^+$), SLAM expression on $CD34^-$/LSK cells was analyzed using anti CD150-VioGreen (TC15-12F12.2, Biolegend) and anti CD48-PE (HM48-1, BD Biosciences). Flt3 expression was tested by anti Flt3-biotynilated (A2F10, Biolegend) together with Streptavidin-APC/Cy7 (Biolegend). For intracellular ROS detection, cells were incubated for 10 min at 37 °C with 2 μM hydroethidine (Life Technologies) prior to cell surface staining for CD34/LSK or αSMA macrophages markers as described above and below. For CMP ($CD34^+/Lin^-/Sca\text{-}1^-/c\text{-}Kit^+/CD16/32^-$) cell surface markers, a lineage cocktail of FITC-conjugated antibodies as described above was used (all from Biolegend)

together with anti Sca-1-PE-Cy7 (D7, BioLegend), anti c-Kit-APC (2B8, Biolegend), anti CD34-eFlour 450 (RAM34, eBiosciences) and anti-CD16/32-PE (93, BioLegend). CLP ($Lin^-/Sca\text{-}1^{low/inter}/c\text{-}Kit^{low/inter}/IL7R\alpha^+$) cell surface markers (Bahr et al., 2018) were determined by staining with a lineage cocktail of FITC-conjugated antibodies as described above was used (all from Biolegend) together with anti Sca-1-PE-Cy7 (D7, BioLegend), anti c-Kit-APC (2B8, Biolegend) and anti-CD127 (IL7Rα)-PE-Cy7 (A7R34, BioLegend). Neutrophils ($CD11b^+/Ly6G^+$) and monocytes ($CD11b^+/Ly6C^+$) were identified by staining with anti-CD11b-FITC (M1/70, BioLegend) and anti-Ly6G-APC (1A8, biogems) or anti-Ly6C-PE-Cy7 (HK1.4, BioLegend). For lymphocyte detection, rat anti mouse CD45R/B220-PE (RA3-6B2, BD Biosciences) was used. TACE levels were detected by anti-TACE (ADAM17) polyclonal antibody (ab39163, Abcam). Levels of cells in G_0 state were determined by staining for cell surface markers of CD34-/LSK as described above or αSMA macrophages markers as described below following fixation and permeabilization and staining with mouse anti-human Ki67-FITC set (556026, BD Biosciences). Detection of αSMA macrophages ($CD11b^+/\alpha SMA^+$) was done by staining for cell surface marker with anti-CD11b-APC (M1/70, eBioscience) following fixation and permeabilization. Then anti- αSMA-FITC monoclonal antibody (1A4, Sigma) was used. Detection of either COX-2 or MT1/MT2 receptors in αSMA macrophages was done after staining for these cells as described above and further using anti-COX-2-unconjugated polyclonal antibody (aa570-598, Cayman chemical company) or anti-MT1-unconjugated polyclonal antibody (Imuny) or anti-MT2 polyclonal antibody (Imuny). Detection of MT1/MT2 receptors in CD34/LSK cells was done after staining for these cells as described above and further using anti-MT1-unconjugated polyclonal antibody (Imuny) or anti-MT2 polyclonal antibody (Imuny). For phosphorylated antibody detection, the bones were maintained on ice followed by flushing and staining on ice. Detection of phosphorylated RelB/p65/Akt were done by staining for cell surface marker for CD34/LSK followed by fixation and permeabilization. Then anti-phosphorylated (Ser552) RelB-PE monoclonal antibody (D41B9, Cell Signaling) or anti-phosphorylated (Ser536) p65-PE monoclonal antibody (93H1, Cell Signaling) or anti-phosphorylated (Thr308) Akt polyclonal antibody (9275S, Cell Signaling) were used. For Lineage (Lin^-) separation a biotinylated lineage cocktail (Miltenyi) was first used followed by anti-biotin microbeads (Miltenyi) according to manufacturer's instructions.

Human HSPC populations were assessed with the following antibodies by flow cytometry on a BD Celesta (from BD Biosciences): FITC-anti-CD45RA, PE-anti-CD90, PE-Dazzle-anti-CD38, BV650-anti-CD49f, APC-anti-CD71, APC-cy7-anti-CD34, AF700-anti-CD10, AF700-anti-CD7, V500-anti-CD45, BV711-anti-CD19 and BV421-anti-CD33. We identified human LT-HSC ($CD34^+CD38^-CD90^+CD45RA^-CD49f^+$), human ST-HSC ($CD34^+CD38^-CD90^-CD45RA^-CD49f^-$) and human MLP ($CD34^+CD38^-CD90^-CD45RA^+$), according to protocol of the Dick lab.

TNF ELISA

Method #1: refers to all TNF measurements except for Fig. 3H.

TNF ELISA was performed by using a mouse TNF ELISA MAX^{TM} Deluxe kit (BioLegend, 430904) according to manufacturer's instructions. Total protein content in BM fluids was quantified by Bradford assay and TNF concentration in the BM fluids was normalized per protein content. Values were expressed as pg/mg protein for BM samples and as pg/ml for plasma samples. The assay has a detection limit of 4pg/ml. The 0pg/ml threshold was set according to plasma TNF KO samples that showed 0pg/ml. However in the plasma we obtain values that are below the ELISA kit sensitivity value and therefore are only suggestive. The 0pg/mg protein threshold for the BM measurements was set according to BM supernatant TNF KO samples. Of note, in the BM there was a false positive background of 3.22pg/mg protein in TNF KO samples thus this value was subtracted from all the TNF levels of WT samples and was set as the point of 0pg/mg protein in all the graphs of BM TNF levels.

Method #2: refers only to Fig. 3H.

TNF ELISA was performed by using the MILLIPLEX MAP Mouse Cytokine/Chemokine Magnetic Bead Panel - Immunology Multiplex Assay (MCYTOMAG-70K, Merck), according to manufacturer's instructions. BM extracellular fluid samples were collected at 7AM and TNF was measured. TNF concentration (pg/ml) was normalized to protein concentration (mg/ml) measured with BCA Protein Assay Kit (Thermo Scientific; #23227). Due to difference in the TNF levels obtain by these two methods, TNF levels in Fig. 3H are expressed as fold change.

Melatonin ELISA

The content of melatonin in plasma and BM fluids was measured through enzyme-linked immunosorbent assays (Melatonin ELISA; IBL, Hamburg, Germany) according to the manufacturer's instructions. Values were expressed as ng/mL and the assay has a detection limit of 3pg/mL.

Competitive repopulation assay

BM cells from C57BL/6 (CD45.2) mice harvested at 11AM or 11PM were transplanted into lethally irradiated (950 cGy) B6.SJL (CD45.1) congenic mice (2×10^5 donor cells collected at the same time with 4×10^5 host cells). BM transplantation was performed 24 h after irradiation. Mice were killed 1 month or 4 months later and the levels of donor chimerism were determined by flow cytometry using rat anti-mouse CD45.2 (BioLegend) and CD45.1 (eBioscience). In the experiments with β3-antagonist, mice were treated with the antagonist at 6AM and 9AM and the BM cells were harvested at 11AM. For the short-term repopulation following melatonin treatment, donor C57BL/6 mice were treated with melatonin at 6AM and sacrificed at 11AM. Donor cells were transplanted

into B6.SJL congenic mice (full dose (x) - 2×10^5 donor cells collected at the same time with 4×10^5 host cells or half dose (1/2x) - 1×10^5 donor cells collected at the same time with 4×10^5 host cells).

Chimera mice establishment

Recipient TNF KO or WT mice were subjected to irradiation (950 cGY) 16-20h before transplantation. BM cells (10×10^6 donor cells) from WT or TNF KO mice was harvested and transplanted as following: WT into TNF KO and TNF KO into WT recipients. Four weeks after transplantation the experiments were conducted by killing the mice at 7AM and comparing their TNF and ROS HSPC levels.

Colony-forming assay (CFU-C)

BM mononuclear (BM-MNC) cells were isolated by Ficoll separation and were seeded ($15x10^3$ cells/ml) in CFU-C semisolid medium supplemented with EPO, IL-3, GM-CSF and SCF as described (Kollet et al., 2006). CFU-C were scored 7 days after plating and presented as CFU-C per number of seeded cells.

***In vivo* Evans Blue dye BM penetration assay**

BM vascular endothelial barrier function was assessed using the Evans Blue Dye (EBD) assay. Evans Blue (Sigma-Aldrich) dissolved with PBS was injected i.v. to mice. For the WT 11AM and 11PM as well as for NE, Luzindole or melatonin treated mice we injected 10mg/ml Evans Blue Dye 5h before mice were euthanized. For β3-antagonist treated mice we injected 20mg/ml Evans Blue Dye 2h before mice were euthanized. In each experiment, a non-injected mouse was used for control blank measurements. Subsequently, mice were perfused with PBS via the left ventricle to remove intravascular dye. Femurs were removed and formamide was used for bone flushing, crushing and chopping. EBD was extracted in formamide by incubation and shaking of flushed and crushed fractions, overnight at 60 °C. Next, we performed 30 min centrifugation at 2,000*g*, EBD in BM supernatants was quantitated by spectrophotometric analysis at 620 nm.

Human lineage depleted cord blood preparation

Human umblical cord blood (CB) samples were obtained from Trillium and Credit Valley Hospital with informed consent according to procedures approved by the University Health Network (UHN) Research Ethics Board. Mononuclear cells were isolated by centrifugation on Lymphoprep medium (Stem Cell Technologies) and depleted of Lineage positive cells (lineage depletion) by negative selection with the StemSep Human Progenitor Cell Enrichment Kit according to the manufacturer's protocol (Stem Cell Technologies). Lin^- CB cells were stored viably at -80°C or -150°C.

In vitro cultures

Fresh bone marrow cells were seeded in RPMI (Gibco) with 10% FCS (Biological Industries), L-glutamine (Biological Industries), penicillin and streptomycin (Invitrogen). For pAKT levels in HSPC: total BM cells were cultured at a density of 2.5 × 106 cells per 1 ml in 12-well plates (Costar) with or without 10nM melatonin for 10min. The cells were taken and stained for pAKT/CD34-LSK. For ROS levels in HSPC, lineage negative (Lin-) cells were obtained from mouse total BM cells by magnetic beads separation (as described in the flow cytometry section). Lin^- cells (5×10^5) were cultured in 24-well plates (Costar) with or without 10nM melatonin for 1h. The cells were taken and stained for ROS/CD34-LSK. Cultures were incubated for the appropriate time at 37 °C in humidified chambers containing 5% CO2.

NE measurements by LC/MS

Method #1: refers to all NE measurements except for Fig. S1G.

Samples preparation: BM cells were flushed with PBS and the cells were incubated for 45min at 37ºC, 5% CO^2. The condition medium of these cells was collected and centrifuged at 4°C for 5 minutes. Plasma was also collected and centrifuged at 4°C for 5 minutes. Then 50µL of each sample was mixed with 10 µL of metabisulfite (stock concentration 50 mM) for preservation. Later standards (NE and deuterated noradrenaline) and 200 µL of pure acetonitrile were added. After vortex and centrifugation at 4°C samples were transferred into fresh tubes. Sodium chloride was added and after centrifugation supernatants were collected. Then 25 µL of tetraborate buffer solution (stock: 0.2M) and 7 µL of 100% Benzoil chloride were added with a subsequent very long and careful vortexing for derivatization. Next, the samples were incubated for 10 minutes and sodium chloride was added to separate water phase from organic phase, and after intensive mixing, short incubation and short spin 100 µL of the upper phase was transferred into the bottles. Finally 25 µL of pure methanol was added. To remove NA from control samples, we performed 48 hours long UV radiation with meanwhile stirring.

Measurements: all the measurements were performed on high resolution ESI-QqTOF system (TripleTOF 5600^+, DuoSpray Ion Source, external ion calibration; AB Sciex) after chromatographic separation (Nexera XR, Shimadzu). The spectrometer was set to MS/MSHR positive mode, spectra in range of 50-650 Da were collected in accumulation time of 150 ms for product ion 482.2 (NE) and 488.2 (NE-d6), at declastering potential (DP) of 60 for both compounds, collision energy (CE) of 15 for NE and of 17 for NE-d6. Ion source parameters (ESI): Ion source gas (GS1) – 40, ion source gas (GS2) – 50, curtain gas (CUR) – 35, source temperature 6000C, ion spray voltage floating – 5500. Chromatographic conditions: mobile phase in gradient of water 0.1% formic acid (A) and acetonitrile 0.1% formic acid (B)- 0-0.5 min 95% A, 6 min – 100% B, 10 min 100% B, 10.1 min – 95% A, 12 min – 95% A. Chromolith Performance RP-18e 100-2 mm column

(Merck) with guard cartridge RP-18e 5-2 mm at 250C.Quantitative analysis we made on MultiQuant (AB Sciex) software, peaks were calculated for product ion signals in range of 464.12-464.17 Da (NE) and 470.15-470.21 (NE-d6).

Method #2: refers only to Fig. S1G.
Aqueous solution (20uL of 1ug/mL) of d_6-norepinephrine (C.D.N. Isotopes, Canada) was added as internal standard to 300uL of the sample medium. The mix was diluted with 3mL of acetonitrile, followed by centrifugation (21,000gx15min). The collected supernatant was evaporated then re-dissolved in 0.1% formic acid (50uL). Derivatization of amine containing metabolites was performed using Aqc reagent, followed by analysis of norepinephrine and d_6-norepinephrine by liquid chromatography–tandem mass spectrometry as described (Boughton et al., 2011; Wolf et al., 2017).

S1P measurement by RP-HPLC
The measurement of sphingosine-1-phosphate was performed by reversed-phase high-performance liquid chromatography (RP-HPLC) with Hewlett-Packard Series 1200 liquid chromatograph. Internal C17S1P standard (Avanti Polar Lipids) and samples were thawed at room temperature. For 100 μL sample volume, 30 μL of the C17S1P internal standard (diluted in 10 mM K_2HPO_4 mixture of methanol (MetOH), pH 7.2) was added. Mixture of standards was prepared as following: 30 μL of internal standard C17S1P (diluted with a mixture of K_2HPO_4:MetOH, pH 7.2) and 30 μL of internal standard C18S1P (diluted in a mixture of K2HPO4:MetOH, pH 7.2). The samples were mixed and supplemented with 1 M NaCl solution up to 1mL volume. After stirring, 1 mL of methanol and 300 mL of concentrated hydrochloric acid were added. After intensive mixing 2 mL of chloroform was added, stirred (20 min, 900 rpm), and centrifuged (3 min, 3500 rpm, 20°C). We transferred separated lower organic phase into a new tube and the upper phase was re-extracted and the lower organic phase was combined with the previously collected one and dried in a vacuum centrifuge for about 45 min at 45 °C. Immediately before the measurements, the dried extracts were dissolved in 130 μL of methanol and 20 μL of OPA mixture. OPA mixture was prepared as following: 5 mg of o-phthalic dialdehyde, 100 μL of methanol, 5 μL of mercaptoethanol and 5 μL of boric acid at pH 10.5. At the same time we prepared a mixture containing 30 μ of internal standard C17S1P and 30 μL of internal standard C18S1P, to which we added 940 μL of a mixture of K_2HPO_4:MetOH, pH 7.2. 600 μL was transferred to a new tube and 75 μL of OPA was added. Samples with OPA were incubated in the dark at room temperature, 20 min and then centrifuged (10 min, 6000 rpm, 20 °C). We obtained clear supernatant which was transferred to a fresh collecting tube, where we added 20 μL of 10 mM K_2HPO_4 buffer, and after incubation (10 min, +4 °C) and centrifugation (5 min, 6000 rpm, 20 °C) the supernatant was transferred into a vial and analyzed. Data were analyzed with HP Chemstation software (Agilent, USA). Separation in the reversed phase column was carried out on a Cosmosil 5 μm C18-ARII column (150 × 4,6) with a 5 μm

C18-ARII (10 × 4.6) pre-column (Waters). Column temperature was 25 °C. The isocratic method with mobile phase consisting of 10 mM K_2HPO_4 (pH 5.5) and methanol (15:85; v/v) was used. The flow rate was 1 mL/min 50 μL samples were injected every 30 min. The wavelength for the detection of S1P derivatives was 340 nm for the excitation and 455 nm for emission. The calculation of S1P concentration was based on the peak area of the internal standard C17-S1P.

- **STATISTICAL ANALYSIS**

All statistical analyses were conducted with Prism 6.0c version (*P<0.05, **P<0.01, ***P<0.001, ****P<0.0001, "ns" represents non significance). All data are expressed as mean ± standard error (s.e.m) and all *n* numbers represent biological repeats. Unless indicated otherwise in figure legends, a Student's two-tailed unpaired t-test was used to determine the significance of the difference between means of two groups. One-way ANOVA was used to compare means among three or more independent groups. Bonferroni or Tukey post-hoc tests were used to compare all pairs of treatment groups when the overall *P* value was <0.05. Animals were randomly assigned to treatment groups.

- **DATA AND SOFTWARE AVAILABILITY**

Download links for software used in this study are provided in the Key Resources Table.

STAR methods

KEY RESOURCES TABLE

REAGENT or RESOURCE	SOURCE	IDENTIFIER
Antibodies		
FITC-Ki67	BD Biosciences	Cat# 556026, RRID:AB_396302
FITC-CD4 (clone GK1.5)	BioLegend	Cat# 100406, RRID:AB_312691
FITC-CD8 (clone 53-6.7)	BioLegend	Cat# 100706, RRID:AB_312745
FITC-B220 (clone RA3-6B2)	BioLegend	Cat# 103206, RRID:AB_312991
FITC-CD11b (clone M1/70)	BioLegend	Cat# 101206, RRID:AB_312789
APC-CD11b-APC (clone M1/70)	eBioscience	Cat# 17-0112-83, RRID:AB_469344
FITC- Gr-1 (clone RB6-8C5)	BioLegend	Cat# 108406, RRID:AB_313371
FITC-Ter119 (clone TER-119)	BioLegend	Cat# 116206, RRID:AB_313707
biotinylated lineage cocktail	Miltenyi	Cat# 130-092-613, RRID:AB_1103214
PE-Sca-1 (clone D7)	BioLegend	Cat# 108108, RRID:AB_313345
Sca-1-PE-Vio770 (clone REA422)	Miltenyi	Cat# 130-106-220
c-Kit-APC (clone 2B8)	BioLegend	Cat# 105812, RRID:AB_313221
eFlour 450-CD34 (clone RAM34)	eBioscience	Cat# 48-0341-82, RRID:AB_2043837
Biotinylated CD34 (clone RAM34)	eBioscience	Cat# 13-0341-82, RRID:AB_466425
Brilliant Violet 510 -CD150- (clone TC15-12F12.2)	BioLegend	Cat# 115929, RRID:AB_2562189
PE-CD48 (clone HM48-1)	BD Biosciences	Cat# 557485, RRID:AB_396725
Biotinylated CD135 (Flt3)	BioLegend	Cat# 135308, RRID:AB_1953267
PE-CD16/32 (clone 93)	BioLegend	Cat# 101307, RRID:AB_312806
PE-Cy7-CD127 (IL7Rα) (clone A7R34)	eBioscience	Cat# A14934, RRID:AB_2534372
APC-Ly6G (clone 1A8)	Biogems, Peprotech	Cat# 83112-80-100
PE-Cy7-Ly6C (clone HK1.4)	BioLegend	Cat# 128018, RRID:AB_1732082
CD45R/B220-PE (clone RA3-6B2)	BioLegend	Cat# 103208, RRID:AB_312993
TACE (ADAM17) rabbit polyclonal antibody	Abcam	Cat# ab39163, RRID:AB_722563
FITC-alphaSMA (clone 1A4)	Sigma	Cat# F3777, RRID:AB_476977
COX-2-unconjugated polyclonal antibody (aa570-598)	Cayman Chemical	Cat# 160106, RRID:AB_10077935
MT1 polyclonal antibody	Imuny	Cat# IM-0482
MT2 polyclonal antibody	Imuny	Cat# IM-0356
Phospho (Ser552) RelB-PE monoclonal antibody (clone D41B9)	Cell Signaling Technology	Cat# 13567
Phospho (Ser536) p65-PE monoclonal antibody (clone 93H1)	Cell Signaling Technology	Cat# 3033
Phospho (Thr308) Akt polyclonal antibody (clone 9275S)	Cell Signaling Technology	Cat# 9275
PE/Cy7-Streptavidin	BioLegend	Cat# 405206
APC/Cy7 Streptavidin	BioLegend	Cat# 405208
Anti-biotin microbeads	Miltenyi	Cat# 130-090-485, RRID:AB_244365

FITC-CD45.1 (clone 104)	BioLegend	Cat#109806
PE-CD45.1 (clone A20)	eBioscience	Cat# 12-4503-83
Anti human FITC- CD45RA	BD Biosciences	Cat# 555488, RRID:AB_395879
Anti human PE- CD90	BD Biosciences	Cat# 555596, RRID:AB_395970
Anti human PE-Dazzle - CD38	BioLegend	Cat# 303538, RRID:AB_2564105
Anti human BV650- CD49f	BD Biosciences	Cat# 563707
Anti human APC- CD71	BD Biosciences	Cat# 551374, RRID:AB_398500
Anti human APC-Cy7- CD34	BD Biosciences	Custom-made
Anti human AF700- CD10	BD Biosciences	Cat# 563509
Anti human AF700- CD7	BD Biosciences	Cat# 561603
Anti human V500- CD45	BD Biosciences	Cat# 560777
Anti human BV711- CD19	BD Biosciences	Cat# 563036
Anti human BV421- CD33	BioLegend	Cat# 303416, RRID:AB_2561690
Biological Samples		
Human cord blood	Trillium and Credit Valley Hospital	
Chemicals, Peptides, and Recombinant Proteins		
Dihydroethidium (Hydroethidine)	Thermo Fisher Scientific	Cat# D1168
TNF	PeproTech	cat # 300-01A
Norepinephrine (NE)	Sigma	cat # A9512
Melatonin	Sigma	cat #M5250
TNF antagonist	Calbiochem	cat #654255
β2 antagonist (ICI)	Sigma	cat # I127
β3 antagonist (SR58894A)	Sigma	cat # SML0581
Luzindole	Sigma	cat #L2407
N-Acetyl Cystein (NAC)	Sigma	cat # A8199
COX-2 inhibitor (NS398)	Sigma	cat #N194
Critical Commercial Assays		
TNF ELISA: MILLIPLEX MAP Mouse Cytokine/Chemokine Magnetic Bead Panel - Immunology Multiplex Assay	Merck	MCYTOMAG-70K
TNF ELISA MAX™ Deluxe kit	BioLegend	Cat#430904
Melatonin ELISA	IBL, Hamburg, Germany	
BCA Protein Assay Kit	Thermo Fisher Scientific	Cat#23227
StemSep Human Progenitor Cell Enrichment Kit	Stem Cell Technologies	Cat#14066
Experimental Models: Organisms/Strains		
Mouse: C57BL/6 (CD45.2)	Harlan/Envigi Laboratories	
Mouse: C3H/HeN	Harlan/Envigo Laboratories	
Mouse: B6.SJL (CD45.1)	Jackson Laboratory	Stock No: 002014
Mouse: TNF KO	Jackson Laboratory	Stock No: 005540

Mouse: Cx3cr1/DTR (cross breeding of Cx3cr1stop-DTR (Jackson Laboratory strain # 025629) to Pgk1-Cre (Jackson Laboratory strain # 020811).	Jackson Laboratory	
Mouse: β2 adrenergic receptor KO (β2AR$^{-/-}$, *Adrb2tm1Bkk/J*),	Jackson Laboratory	Stock No: 003810
Mouse: β3 adrenergic receptor KO (β3AR$^{-/-}$, *Adrb3^{tm1Lowl}*)	Jackson Laboratory	Stock No: 006402
Mouse: double KO of β2 and β3 adrenergic receptors (β2AR$^{-/-}$/ β3AR$^{-/-}$)		
Mouse: NSG; NOD.Cg *Prkdc*scid*Il2rg*tm1Wjl /SzJ females	Jackson Laboratory	Stock No: 005557
Mouse: NSG-SGM3; NOD.Cg-Prkdcscid Il2rgtm1Wjl Tg(CMV-IL3,CSF2,KITLG)1Eav/MloySzJ females	Jackson Laboratory	Stock No: 013062
Software and Algorithms		
MacsQuantify	Miltenyi	
FlowJo	FlowJo	
Prism	GraphPad Software	https://www.graphpad.com/scientificsoftware/prism/
Adobe Illustrator	Adobe	https://www.adobe.com/de/products/ illustrator

Figure 1

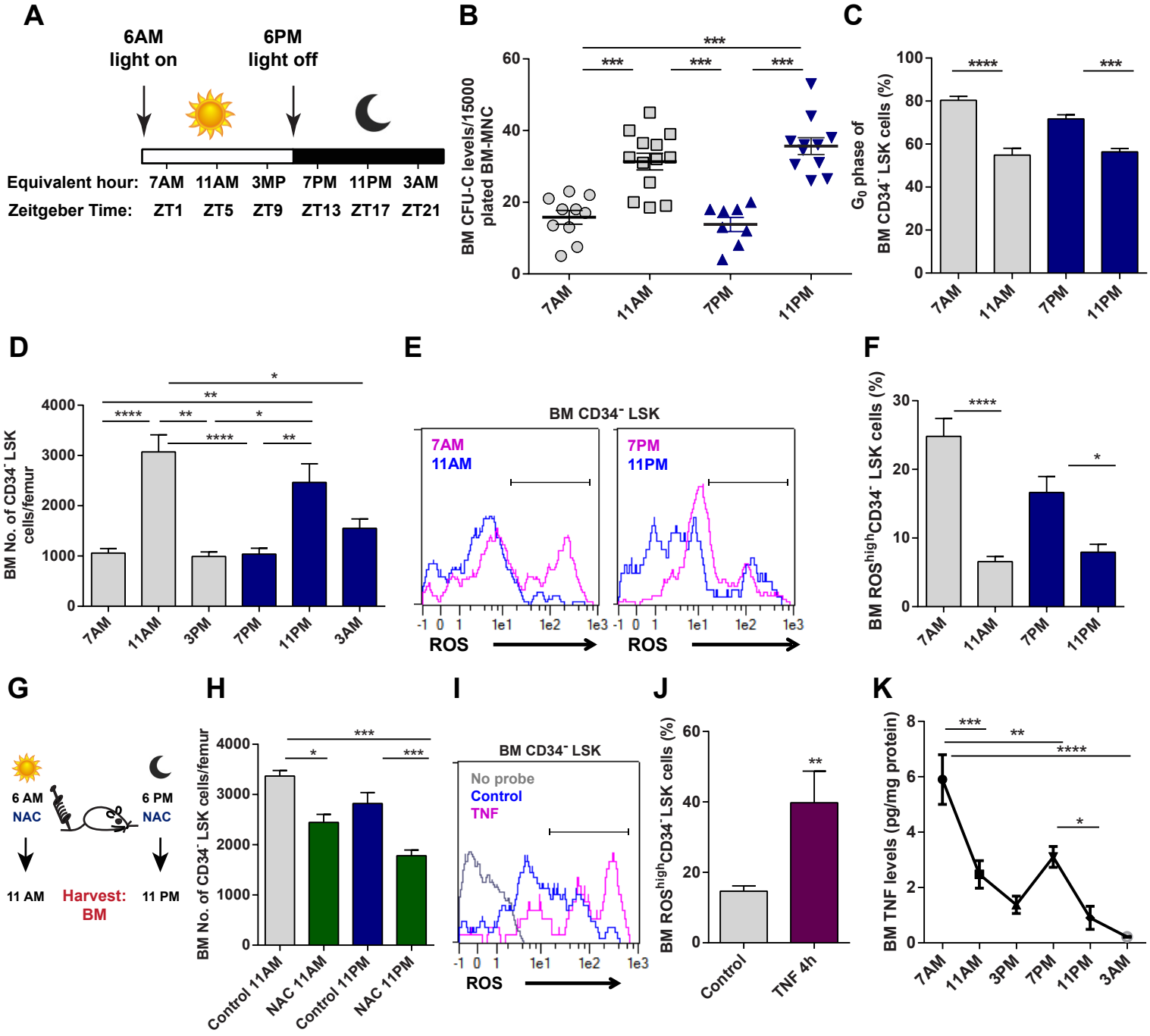

Figure 1: Light and darkness cues induce two peaks of BM HSPC proliferation via TNF and ROS production.

Figure 2

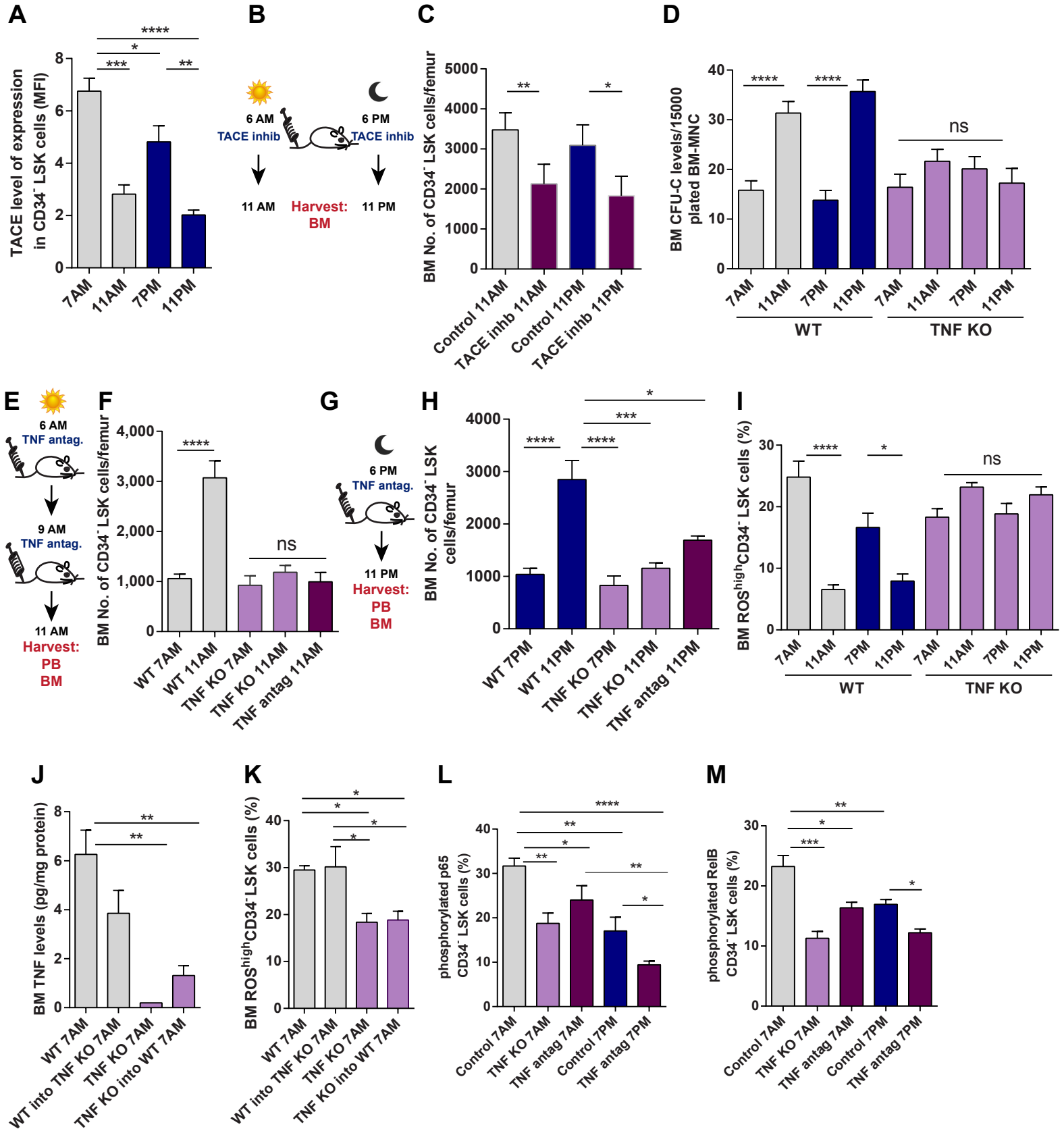

Figure 2: TNF is essential for HSPC BM peaks induction.

Figure 3

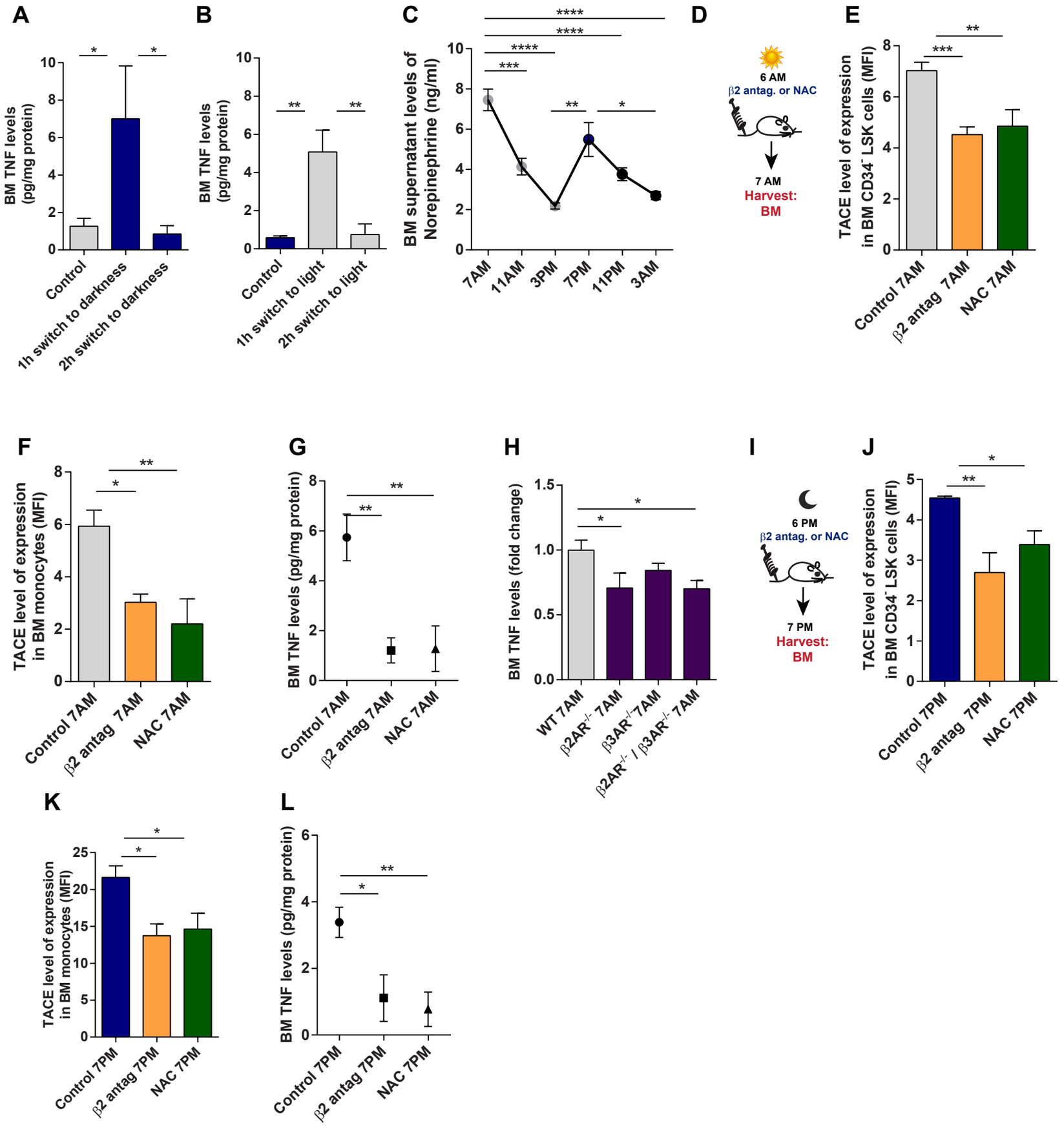

Figure 3: TNF is transiently elevated via NE secretion following light/dark onset.

Figure 4

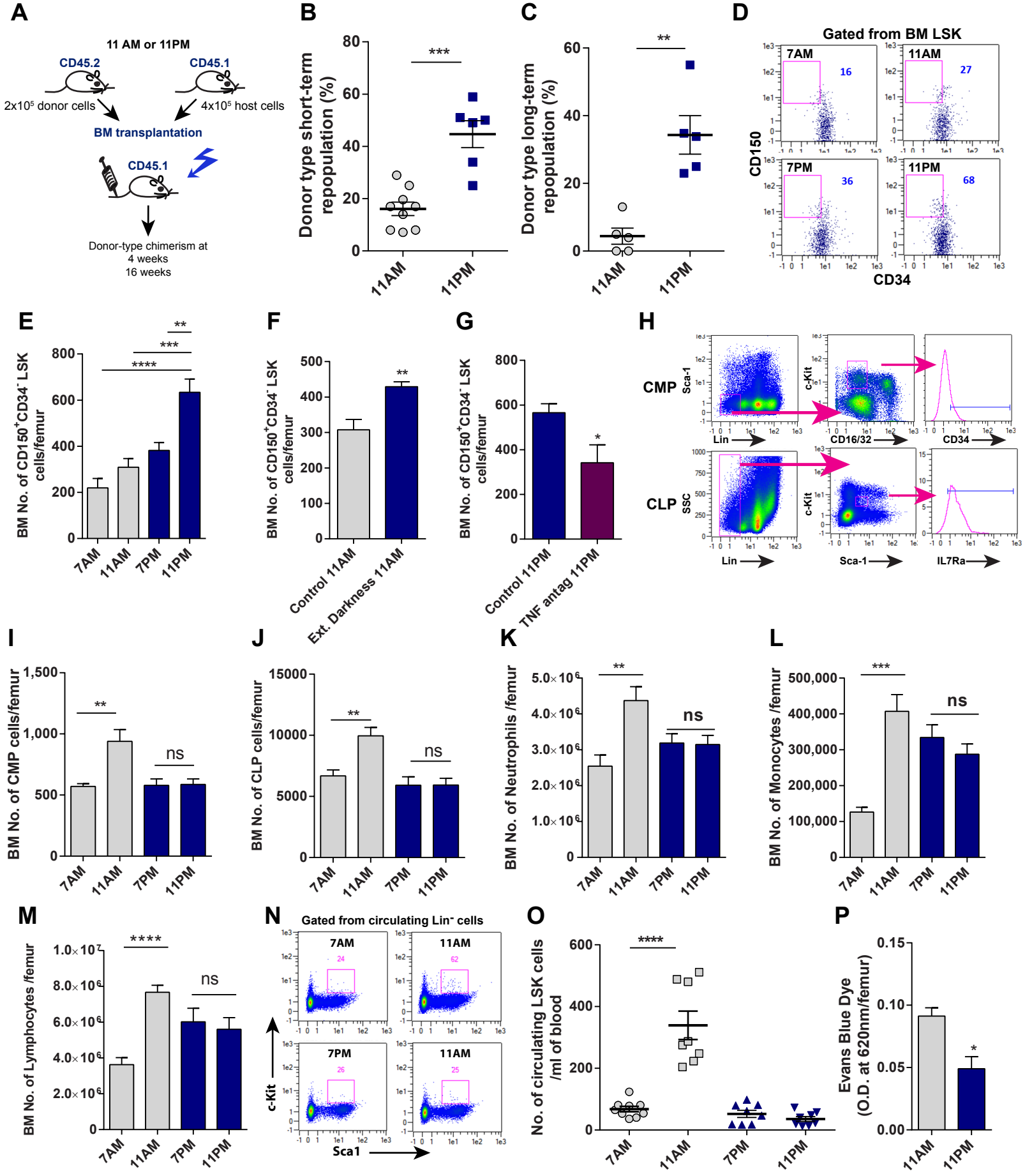

Figure 4: The daylight peak involves HSPC increased egress and differentiation while the night peak consists of HSPC retention and reduced differentiation.

Figure 5

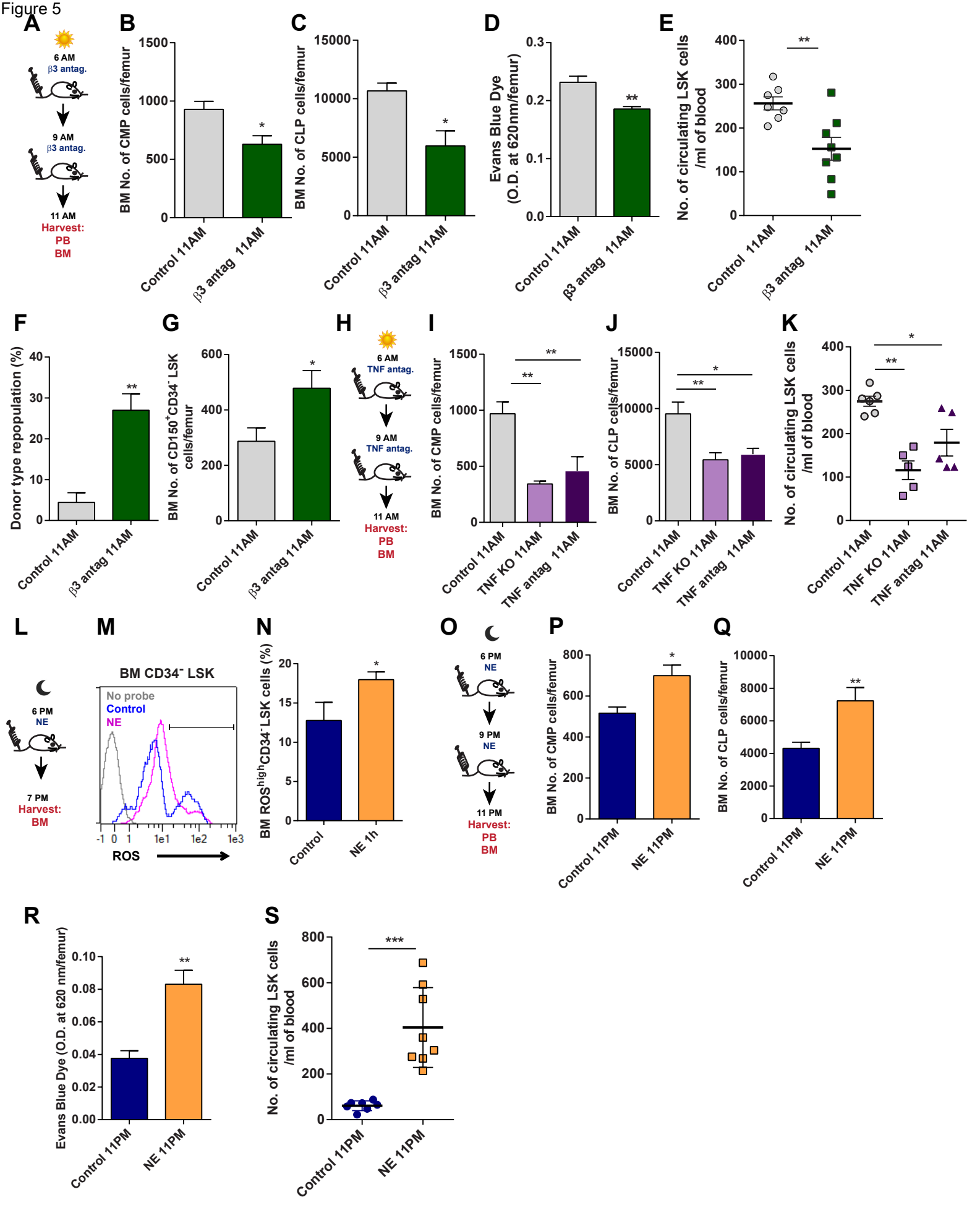

Figure 5: Elevated morning NE further increases ROS levels and vascular permeability leading to HSPC egress and differentiation.

Figure 6

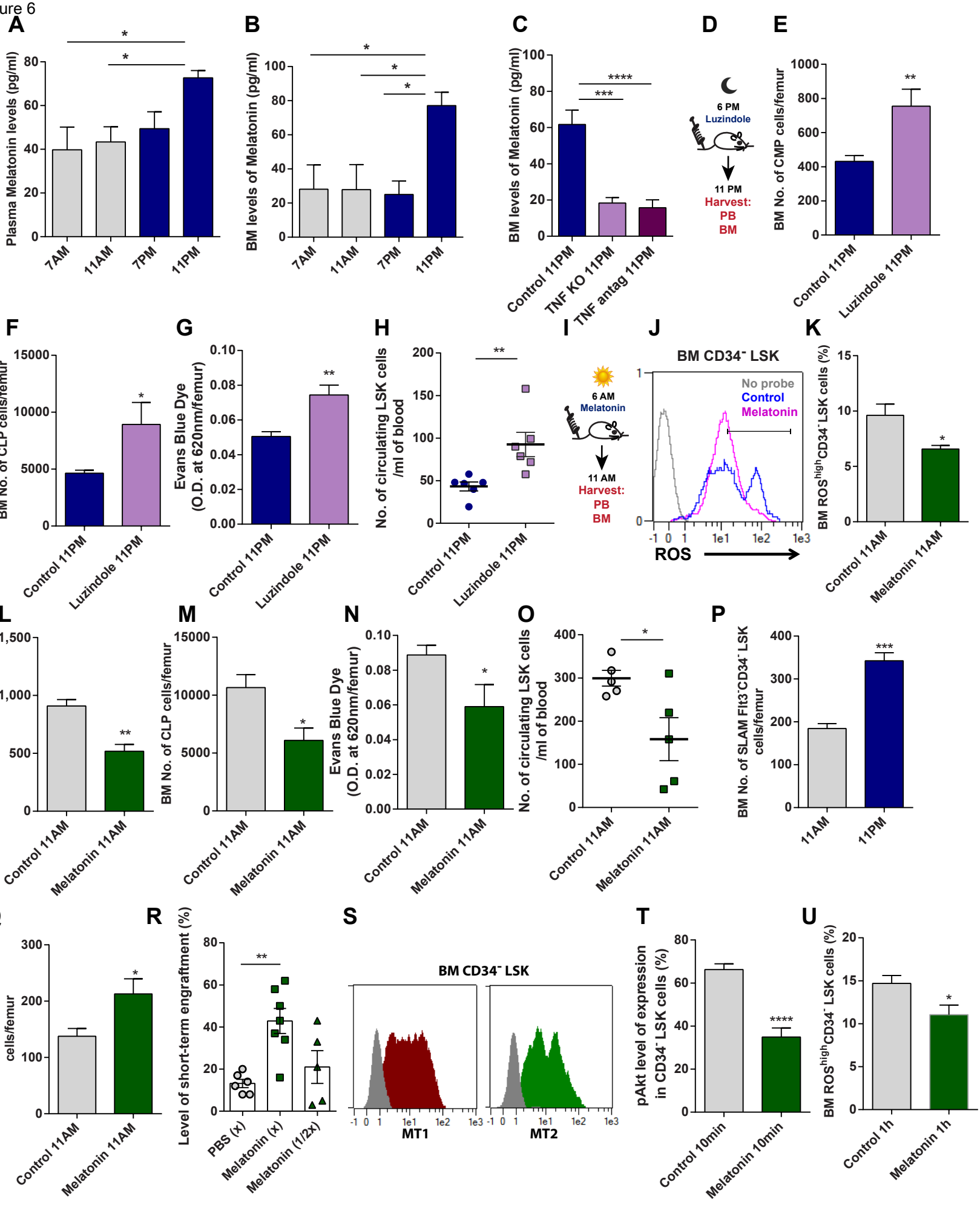

Figure 6: During the night, augmented melatonin levels maintain HSPC undifferentiated and retained in the BM.

Figure 7

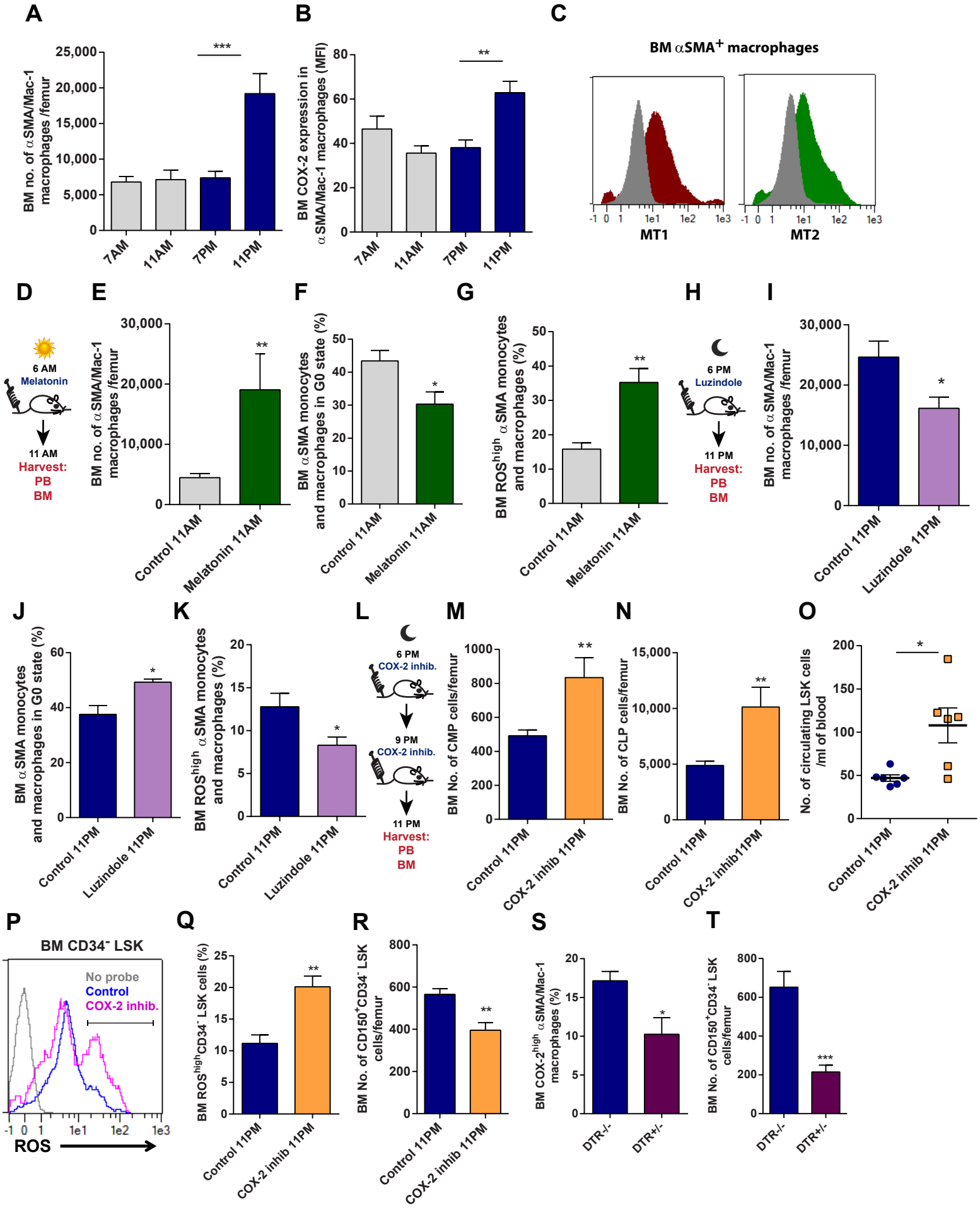

Figure 7: Melatonin-induced elevation of COX-2/αSMA macrophages indirectly reduced HSPC egress and differentiation.

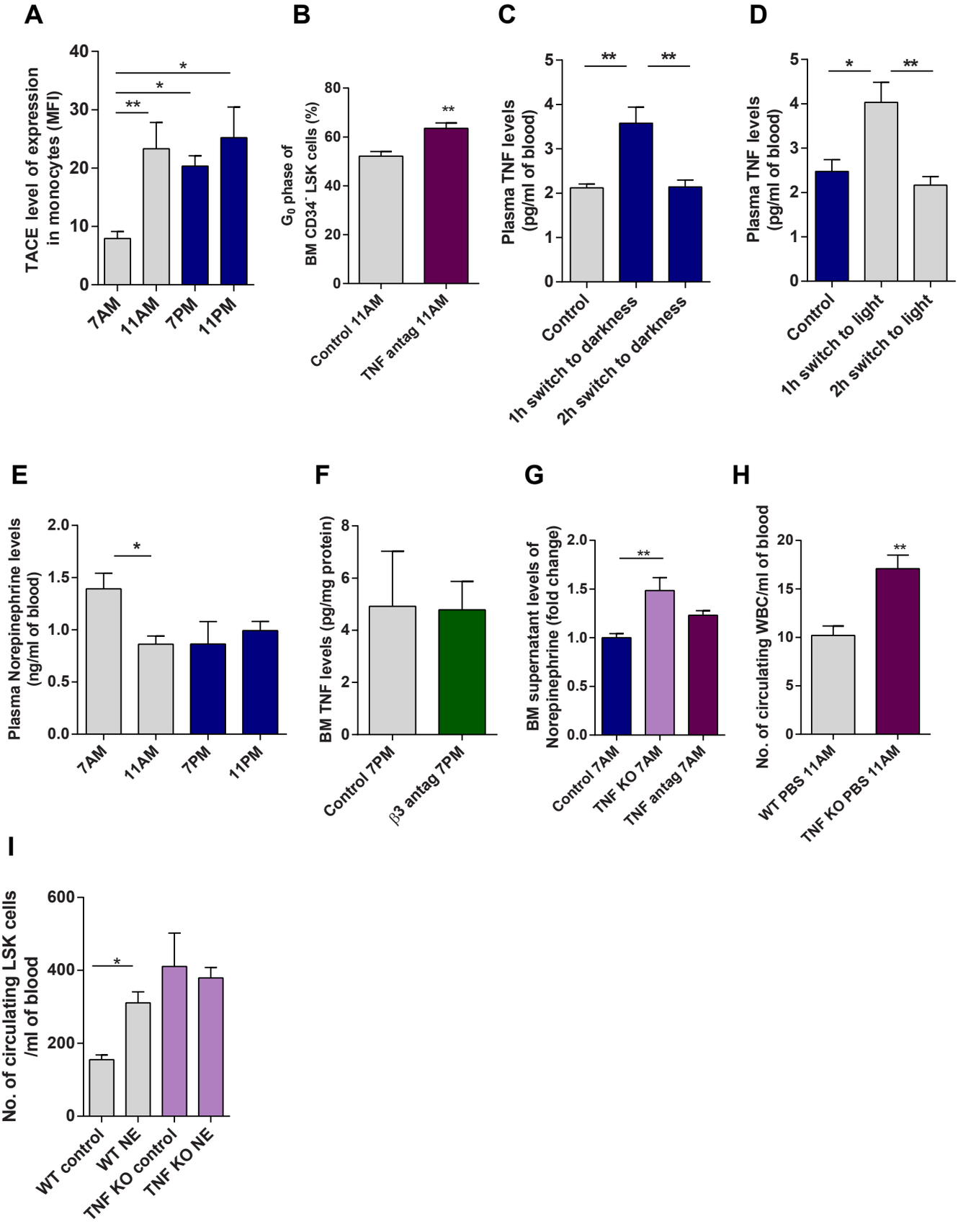

Figure S1. Relates to figure 2 and Figure 3: Mutual cross talk between NE and TNF regulate BM HSPC peaks.

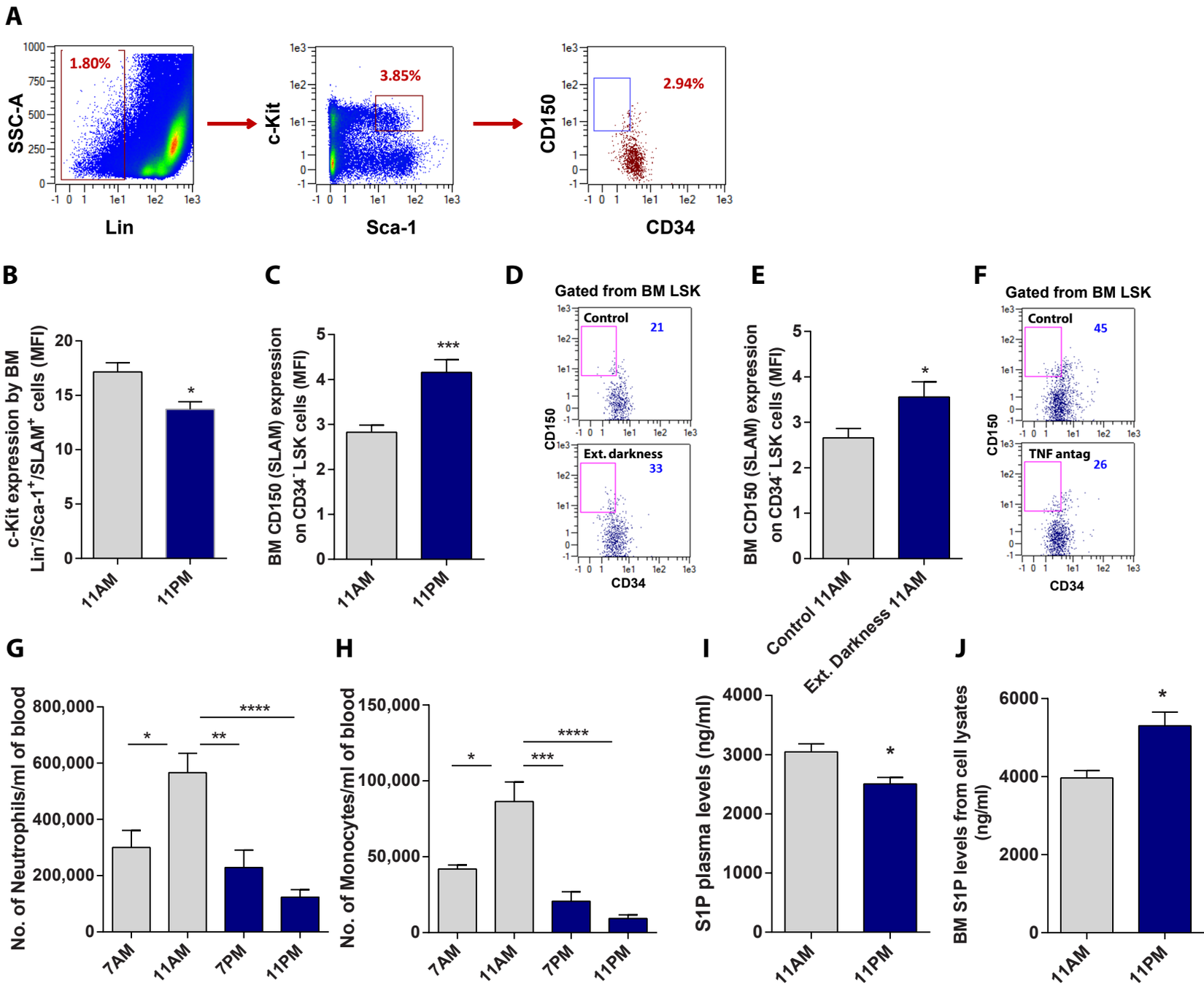

Figure S2. Relates to figure 4: BM cells primed for an immature phenotype at night. Egress of neutrophils and monocytes to the circulation peaks at 11AM, a time of increased S1P in the plasma.

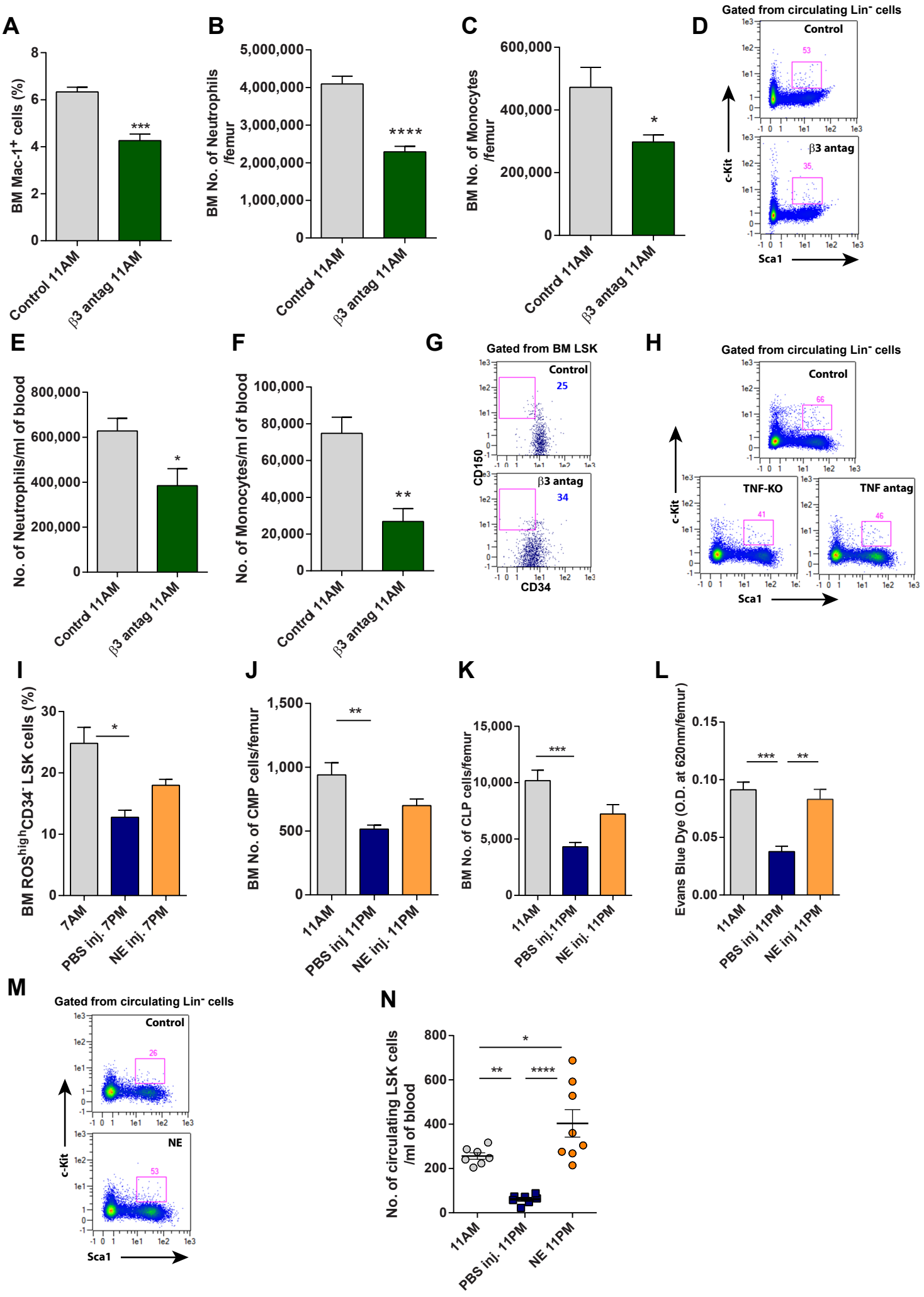

Figure S3. Relates to figure 5: Reducing NE activity in the morning by β3 antagonist decreased differentiation and egress while administration of NE at night increased differentiation and egress.

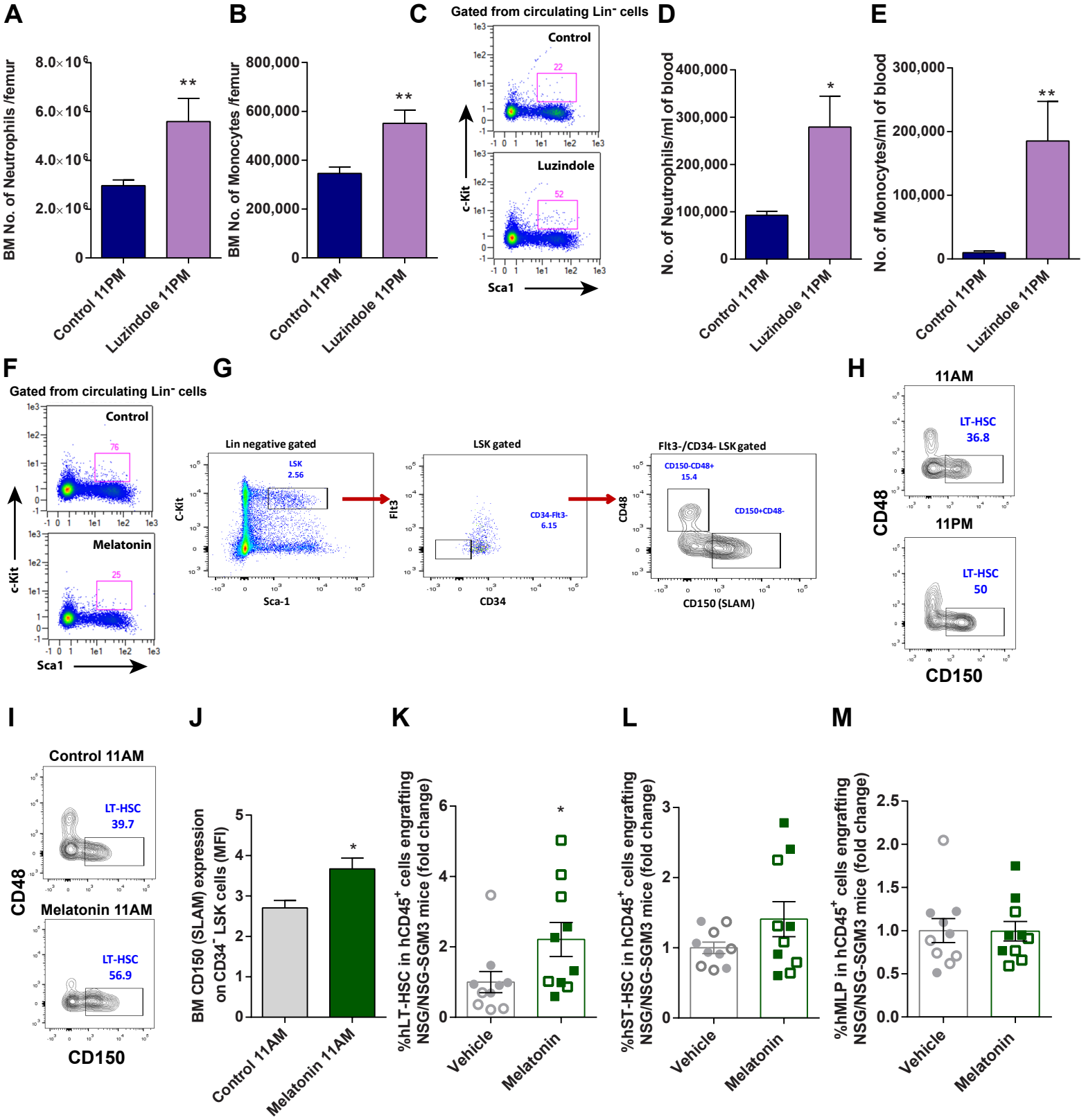

Figure S4. Relates to figure 6: Inhibition of Melatonin at the night peak induced differentiation to mature neutrophils and monocytes in the BM and their egress to the circulation. Melatonin injection in the morning enhances HSC penotype.

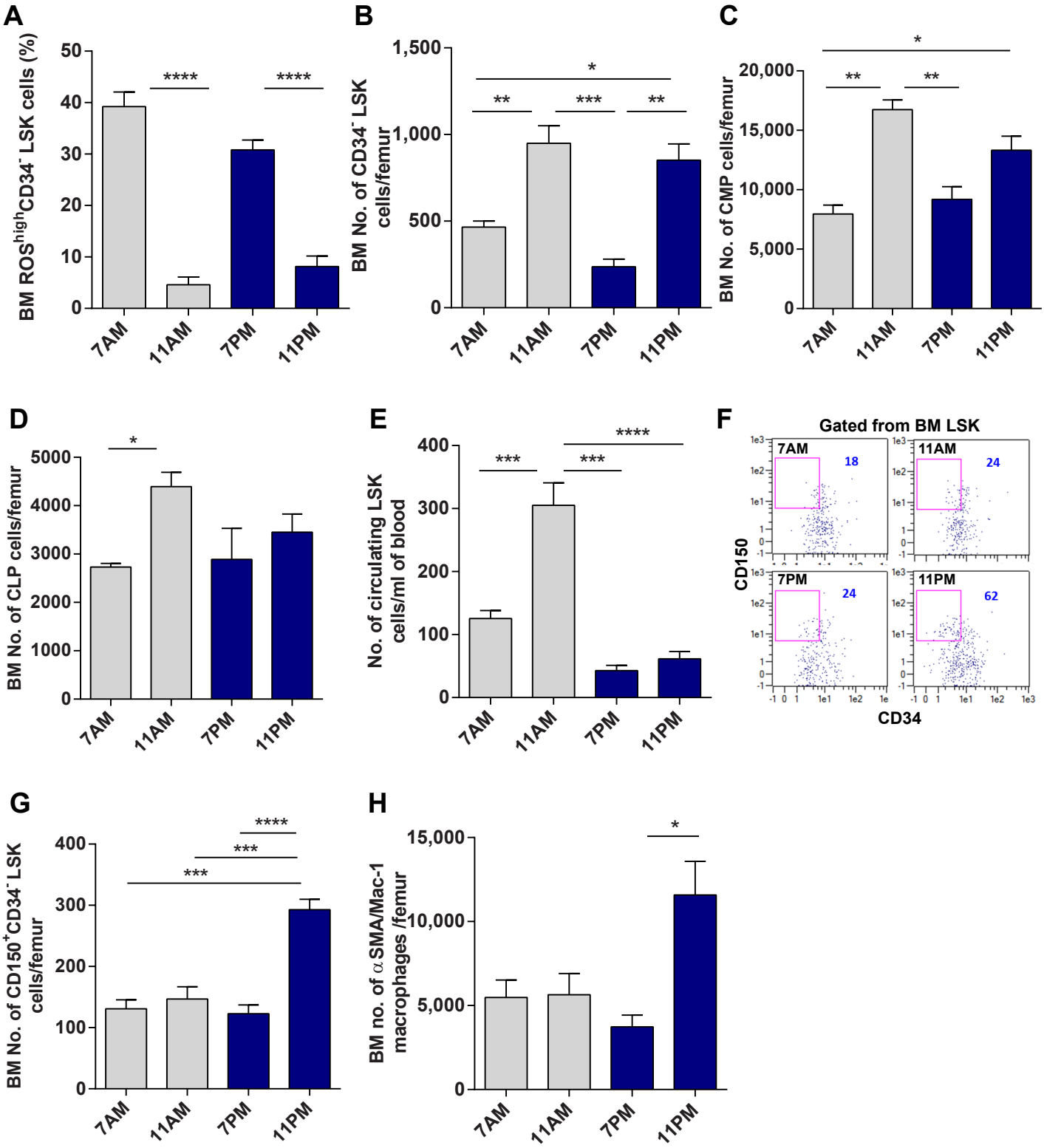

Figure S5. Relates to figure 6 and figure 7: C3H mice display daily fluctuations similar to C57BL/6 mice.

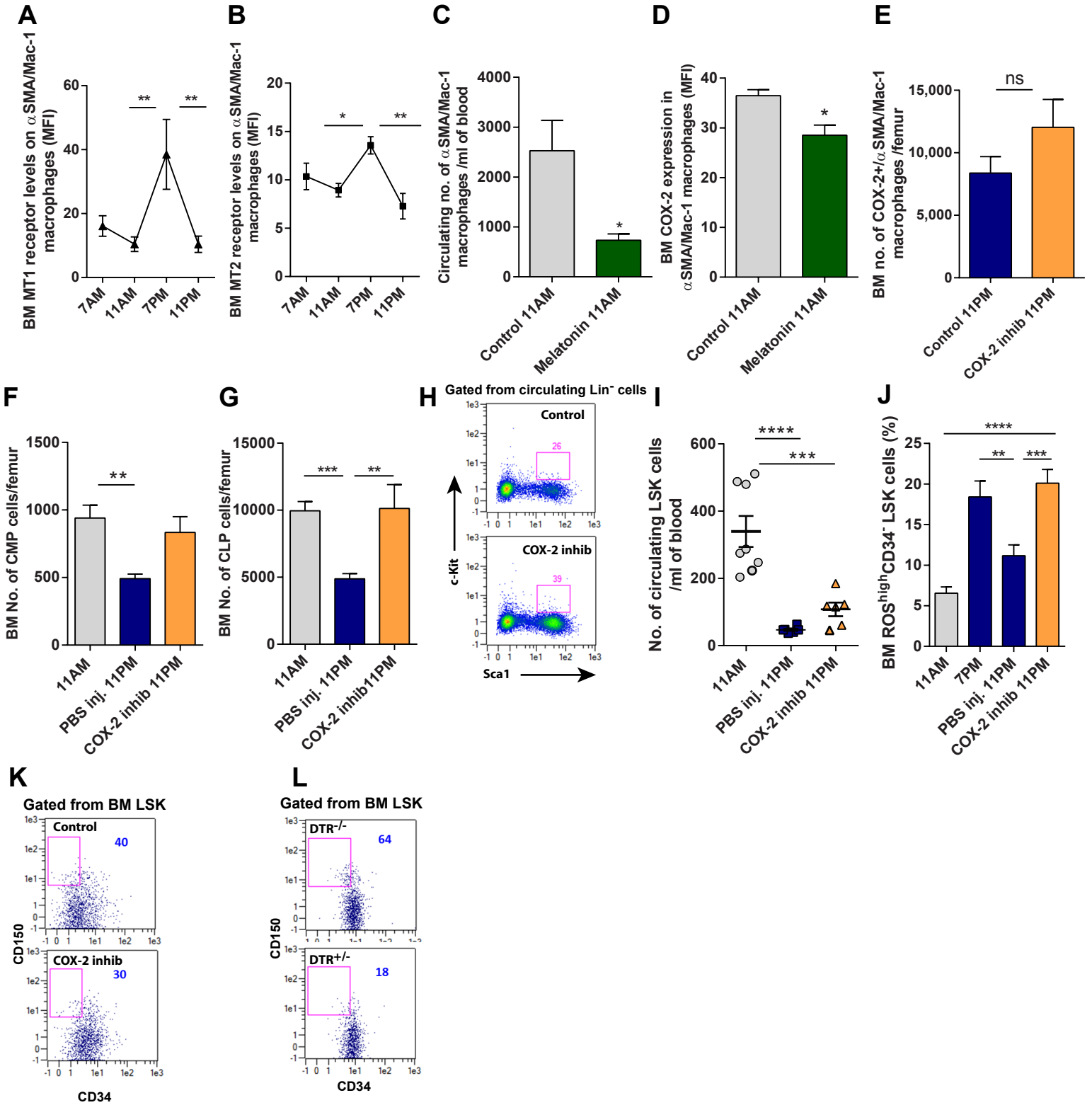

Figure S6. Relates to figure 7: Cox-2/αSMA^{+} macrophages are important regulators of HSPC maintenance at night.

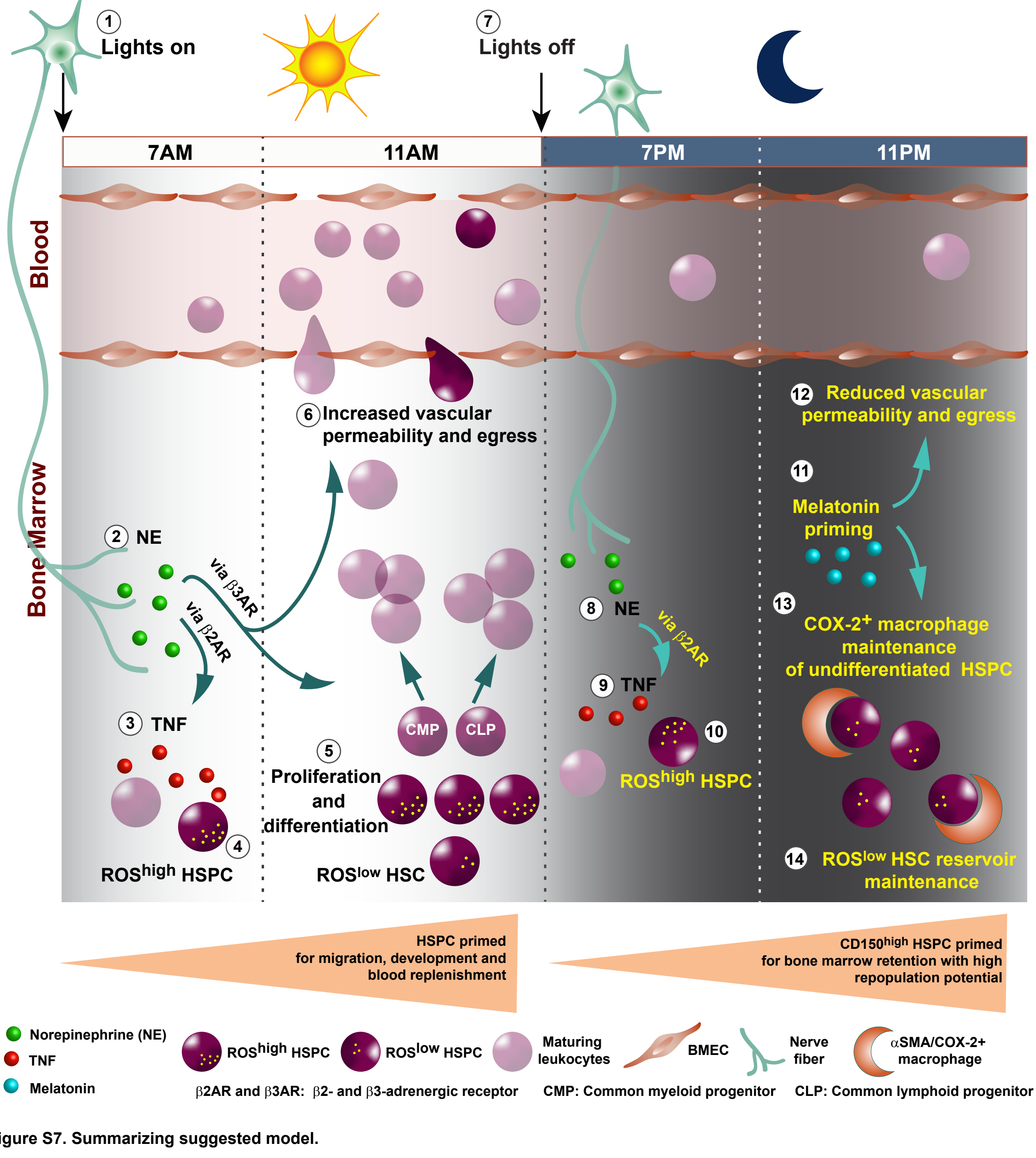

Figure S7. Summarizing suggested model.

Figure S1 related to Figure 2 and Figure 3: **A mutual cross talk between NE and TNF. (A)** BM TACE level of expression in monocytes (*n* = 5). **(B)** Percentage of quiescent G_0 stage of BM $CD34^-$/LSK cells at 11PM following TNF antagonist administration (*n* = 4). **(C)** TNF levels in the plasma (*n* = 5) following 1h or 2h switch from light to darkness. **(D)** TNF levels in the plasma (*n* = 4) following 1h or 2h switch from darkness to light. **(E)** NE levels in the plasma (*n* = 7) at different time points of the day. **(F)** TNF levels in the BM (*n* = 3) at 7AM following β3AR antagonist administration. **(G)** NE levels in the BM (*n* = 6) at 7AM in TNF KO mice and following TNF antagonist administration. The results are represented as fold change. **(H)** Numbers of circulating white blood cells (WBC) in WT and TNF KO mice following injection with PBS (*n* = 4). **(I)** Numbers of circulating LSK in WT and TNF KO mice following injection with NE for 1h (mice were injected at 2PM) (*n* = 4). Error bars, mean ± s.e.m. *P < 0.05; **P < 0.01, Student's two-tailed unpaired t-test (B, F, H), one-way ANOVA with Tukey's *post hoc* test (A, C-E, G, I).

Figure S2 related to Figure 4: **BM cells primed for an immature phenotype at night. Egress of neutrophils and monocytes to the circulation peaks at 11AM, a time of increased S1P in the plasma. (A)** Gating strategy for $CD150^+/CD34^-$/LSK cells in the BM. **(B)** c-Kit level of expression on $Lin^-/Sca\text{-}1^+/CD150^+$ cells in the BM (*n* = 3). **(C)** $CD150^{high}$ level of expression on $CD34^-$/LSK cells in the BM (*n* = 8). **(D)** FACS representative plots of the number of BM $CD150^+/CD34^-$/LSK cells at 11AM following extended darkness. **(E)** $CD150^{high}$ level of expression on $CD34^-$/LSK cells in the BM at 11AM following extended darkness (*n* = 5). **(F)** FACS representative plots of the number of BM $CD150^+/CD34^-$/LSK cells following TNF antagonist administration. **(G-H)** Numbers of circulating neutrophils (E, *n* = 7) and monocytes (F, *n* = 6) per ml of blood. **(I-J)** S1P levels in the plasma (G, *n* = 6) and in the BM (H, *n* = 4) at 11AM and 11PM. Error bars, mean ± s.e.m. *P < 0.05; **P < 0.01; ***P < 0.001; ****P < 0.0001, Student's two-tailed unpaired t-test (A, C, G-H), one-way ANOVA with Tukey's *post hoc* test (E-F).

Figure S3 related to Figure 5: **Reducing NE activity in the morning decreased HSPC differentiation and egress, while administration of NE at night induced differentiation and egress. (A-C)** Percentage of Mac-1$(CD11b)^+$ cells (A, *n* = 5), numbers of BM neutrophils (B, *n* = 7) and monocytes (C, *n* = 6) per femur following β3AR antagonist administration. **(D)** FACS representative plots of circulating LSK cells following β3AR antagonist administration. **(E-F)** Numbers of circulating neutrophils (E, *n* = 7) and monocytes (F, *n* = 6) per ml of blood following β3AR antagonist administration. **(G)** FACS representative plots of BM $CD150^+/CD34^-$/LSK cells following β3AR antagonist administration. **(H)** FACS representative plots of circulating LSK cells in TNF KO mice and following TNF antagonist administration to WT mice. **(I-N)** Percentage of ROS^{high}

CD34$^-$LSK cells in the BM at 7PM following NE 1h administration compared to 7AM steady state levels (I). **N**umber of BM CMP (J, *n* = 5) or CLP (K, *n* = 6) cells per femur, Evans Blue Dye absorbance per femur at 620nm (L, *n* = 4) and circulating LSK cells: representative plots (M) and data summarized per ml of blood (N, *n* = 8) at 11PM in NE treated mice compared to 11AM steady state levels. Error bars, mean ± s.e.m. *P < 0.05; **P < 0.01; ***P < 0.001; ****P < 0.0001, Student's two-tailed unpaired t-test (A-C, E-F), one-way ANOVA with Tukey's *post hoc* test (I-N).

Figure S4 related to Figure 6: **Inhibition of Melatonin during the night increased differentiation and mature leukocyte egress. (A-B)** Numbers of BM neutrophils (A, *n* = 6) and monocytes (B, *n* = 5) per femur following luzindole administration. **(C)** FACS representative plots of circulating LSK cells at 11PM following luzindole administration. **(D-E)** Numbers of circulating neutrophils (D, *n* = 6) and monocytes (E, *n* = 4) per ml of blood following luzindole administration. **(F)** FACS representative plots of circulating LSK cells at 11AM following melatonin administration. **(G)** Gating strategy for Flt3$^-$/CD34$^-$/SLAM/LSK LT-HSC in the BM. **(H-I)** FACS representative plots of BM Flt3-/CD34-/SLAM/LSK LT-HSC at 11AM and 11PM (H) and at 11AM following melatonin administration (I). **(J)** CD150^{high} level of expression on CD34$^-$/LSK cells in the BM at 11AM following melatonin administration (*n* = 5). **(K-M)** NSG (solid symbols), and NSG with human growth factors (NSG-SGM3) (open symbols) xenogeneic mice transplanted with human cord blood cells were treated with melatonin at 6AM and the percentage of LT-HSC (K, *n* = 5 each), ST-HSC (L, *n* = 5 each) and MLP (M, *n* = 5 each) were tested at 10AM. Error bars, mean ± s.e.m (A-J) mean ± SD (K-M). *P < 0.05; **P < 0.01, Student's two-tailed unpaired t-test.

Figure S5 related to Figure 6 and Figure 7: **C3H/HeN mice display daily fluctuations similar to C57BL/6 mice. (A)** Percentage of ROS^{high} CD34$^-$LSK cells in the BM (*n* = 4). **(B)** Numbers of BM CD34$^-$/LSK cells per femur (*n* = 4). **(C)** Numbers of BM CMP cells per femur (*n* = 4). **(D)** Numbers of BM CLP cells per femur (*n* = 4). **(E)** Numbers of circulating LSK cells (*n* = 4). **(F-G)** FACS representative plots (F) and numbers of BM CD150$^+$/CD34$^-$/LSK cells per femur (*n* = 4). **(H)** Numbers of BM αSMA/Mac-1 macrophages per femur (*n* = 4). Error bars, mean ± s.e.m. *P < 0.05; **P < 0.01; ***P < 0.001; ****P < 0.0001, one-way ANOVA with Tukey's *post hoc* test.

Figure S6 related to Figure 7: **COX-2 αSMA macrophages are important regulators of HSPC maintenance at night. (A-B)** Levels of MT1 (A, *n* = 5) and MT2 (B, *n* = 5) melatonin receptor expression in BM αSMA/Mac-1 macrophages. **(C)** Numbers of circulating αSMA/Mac-1 macrophages at 11AM following melatonin administration (*n* = 4). **(D)** Level of COX-2 expression in αSMA/Mac-1 macrophages (*n* = 4) at 11AM following melatonin administration. **(E)** Numbers of BM COX-2/αSMA/Mac-1

macrophages per femur at 11PM following COX-2 inhibitor administration (n = 4). **(F-I) N**umber of BM CMP (F, n = 4) or CLP (G, n = 6) cells per femur and circulating LSK cells: representative plots (H) and data summarized per ml of blood (I, n = 6) at 11PM in COX-2 inhibitor treated mice compared to 11AM steady state levels. **(J)** Percentage of ROS^{high} $CD34^{-}$LSK cells in the BM at 11PM following COX-2 inhibitor treatment as compared to 7PM and 11AM steady state levels (n = 5). **(K)** FACS representative plots of BM $CD150^{+}/CD34^{-}$/LSK cells at 11PM following COX-2 inhibitor administration. **(L)** FACS representative plots of BM $CD150^{+}/CD34^{-}$/LSK cells at 11PM following 12h depletion of Cx3cr1 monocyte and macrophages in DTR mice. Error bars, mean ± s.e.m. *P < 0.05; **P < 0.01; ***P < 0.001; ****P < 0.0001, Student's two-tailed unpaired t-test (C-E), one-way ANOVA with Tukey's *post hoc* test (A-B, F-J).

Figure S7: **Suggested model.** Upon light induction (1), there is a high elevation in BM NE levels (2) leading to TNF augmentation (3) via β2AR on HSPC and monocytes. Together, NE and TNF increase ROS levels in HSPC (4), known to exert their proliferation, differentiation and egress to the circulation (5). At the same time NE further elevates BM vessel permeability via β3AR to facilitate mature and immature cell egress at 11AM (6). Thus the morning peak involves proliferation, differentiation and egress with high BM blood vessel permeability, all associated with a state of increased migration, development and blood replenishment. Following termination of light (7) NE (8), TNF (9) and ROS (10) are elevated, however to a lower extent then in the morning, enabling proliferation without differentiation and egress of HSPC. More importantly, nocturnal melatonin levels are elevated in the BM (11). Melatonin decreases vascular permeability (12) and elevates COX-2/αSMA macrophages (13). As such, melatonin primes HSPC to a state of retention, reduced differentiation and higher CD150 surface expression and repopulation potential (14).